Technische Universität Chemnitz

Sonderforschungsbereich 393

Numerische Simulation auf massiv parallelen Rechnern

Gerd Kunert

A posteriori error estimation for convection dominated problems on anisotropic meshes

Preprint SFB393/02-04

Abstract

A singularly perturbed convection–diffusion problem in two and three space dimensions is discretized using the streamline upwind Petrov Galerkin (SUPG) variant of the finite element method. The dominant convection frequently gives rise to solutions with layers; hence anisotropic finite elements can be applied advantageously.

The main focus is on *a posteriori* energy norm error estimation that is robust in the perturbation parameter and with respect to the mesh anisotropy. A residual error estimator and a local problem error estimator are proposed and investigated.

The analysis reveals that the upper error bound depends on the alignment of the anisotropies of the mesh and of the solution. Hence *reliable* error estimation is possible for suitable anisotropic meshes. The lower error bound depends on the problem data via a local mesh Peclet number. Thus *efficient* error estimation is achieved for small mesh Peclet numbers.

Altogether, error estimation approaches for isotropic meshes are successfully extended to anisotropic elements. Several numerical experiments support the analysis.

Keywords: error estimator, anisotropic solution, stretched elements, convection diffusion equation, singularly perturbed problem

AMS: 65N15, 65N30, 35B25

Preprint-Reihe des Chemnitzer SFB 393

SFB393/02-04 **March 2002**

Contents

Gerd Kunert
TU Chemnitz
Fakultät für Mathematik
09107 Chemnitz
Germany

http://www.tu-chemnitz.de/~gku
http://www.tu-chemnitz.de/sfb393/

1 Introduction

Our work deals with the singularly perturbed diffusion–convection–reaction problem

$$\left.\begin{aligned} -\varepsilon\Delta u + \underline{b}\cdot\nabla u + cu &= f && \text{in } \Omega \\ u &= 0 && \text{on } \Gamma_{\mathrm{D}} \\ \varepsilon\partial_n u &= g && \text{on } \Gamma_{\mathrm{N}}. \end{aligned}\right\} \tag{1}$$

Such problems arise e.g. when linearizing the Navier–Stokes equations. The convection dominated case is particularly interesting, and thus the diffusion parameter is supposed to be small, $0 < \varepsilon \ll 1$. As a consequence, the solution u of (1) frequently has exponential (or regular) boundary layers of width $\mathcal{O}(\varepsilon|\ln\varepsilon|)$, or parabolic (or characteristic) boundary layers of width $\mathcal{O}(\sqrt{\varepsilon}|\ln\sqrt{\varepsilon}|)$. Standard numerical methods such as the Finite Element Method (FEM) or the Finite Difference Method usually fail for small ε since they introduce nonphysical oscillations. One possible remedy involves additional stabilisation. The most successful approaches are the *streamline upwind Petrov Galerkin* method (SUPG), also known as *streamline diffusion finite element method* (SDFEM), the *Galerkin least squares* approximation (GLS), and the *Douglas–Wang* method. Among the extensive literature, we refer to the overview work of [RST96] and [Mor96], and to [HL98] for a unified presentation of stabilized Galerkin methods.

In our work we are solely concerned with the SUPG variant of the finite element method. This includes the analysis of the standard (unstable) Galerkin method when omitting any stabilisation.

Our main interest is in reliable and efficient *a posteriori* error estimators. This topic is by now well understood for symmetric, elliptic partial differential equations (PDEs) where tight upper and lower error bounds are achieved, cf. the overview work of [Ver96, AO00]. For the *convection dominated* case as considered here, the theory is much less mature. This is mainly caused by the large convection which implies a gap between the ellipticity constant and the boundedness constant of the bilinear form associated with the PDE. Hence the constants in the error bounds depend on the problem parameters. Reliability and/or efficiency of the error estimator may be affected adversely.

The last decade has seen much effort to diminish the influence on the problem data. Angermann [Ang95] was the first to eliminate this dependence completely. Unfortunately the error is measured there in a complicated norm which is defined implicitly via an infinite dimensional variational problem. Hence tight error bounds are achieved on the expense of a norm that is difficult to evaluate.

A more feasible approach is presented by Verfürth [Ver98a] and Kay/Silvester [KS01] which measure the error in the energy norm and the H^1 seminorm, respectively. In both cases the error estimator is *reliable*, i.e. an upper error bound holds. The *efficiency* is associated with the lower error bound and depends on a local mesh Peclet number, cf. Section 4 for details.

Formaggia at al. [FPZ01] propose a post–processing based error estimator that employs the dual solution. Recently Sangalli [San01] obtained an error estimate in a particular norm

for the so–called residual free bubble method. Also worth mentioning is the numerical study of *a posteriori* error estimators by John [Joh00]. He compares several estimators that are either heuristically derived or mathematically analysed. There valuable conclusions are obtained about reliability of estimators and their suitability for adaptive algorithms. One (slightly surprising) observation is that parabolic layers can be more difficult to treat than exponential layers.

Finally, a maximum norm *a posteriori* estimator for a 1D problem has been proposed recently in [Kop01]. We also mention the vast literature on *a priori* estimates, cf. [Ape99, RST96] and the citations therein.

The singularly perturbed nature of the convection–diffusion problem frequently gives rise to boundary layers. These layers have strong *anisotropic* behaviour, i.e. they exhibit lower–dimensional features. Problems with anisotropic solutions can be favourably resolved using *anisotropic meshes*. By this we mean meshes with elements whose aspect ratio is not bounded, as in the conventional theory, but can be arbitrarily large. For further reference we refer to Apel [Ape99]; see e.g. also [Kun99, HL98, LS01]. As a consequence of using anisotropic elements, the whole theory of *a priori* and *a posteriori* error estimators has to be reinvestigated since the large aspect ratio influences the error bounds adversely.

Here we are chiefly concerned about *a posteriori* estimators for anisotropic elements. There has been some development in recent years; exemplarily we mention [DGP99, Kun00, Kun01c, Sie96]. There is a common feature of all those estimators that is different to the isotropic theory. Namely, the reliability and efficiency of the error estimator is not achieved for *arbitrary* anisotropic meshes (i.e. independent of the anisotropic solution). If the anisotropy of the mesh and of the solution are well aligned then tight upper and lower error bounds are obtained. Otherwise there can be an arbitrarily large gap between both error bounds, and the error estimator would be useless. For more details see Section 3.3.

In this work we derive and analyse *a posteriori* error estimators that are suitable for singularly perturbed convection–diffusion problems on anisotropic meshes. Our proposals are inspired by estimators for convection–diffusion problems [KS01, Ver98a] and by estimators for anisotropic elements [Kun01b, Kun01c]. It turns out that the *upper error bound* depends on the alignment of the anisotropic mesh and of the anisotropic solution. This dependence enters in the same way as for the Poisson equation or reaction–diffusion equations, cf. [Kun00, Kun01c]. The *lower error bound* involves a local mesh Peclet number Pe_T. It implies *efficiency* of the error estimator if the mesh Peclet number is small ($\mathrm{Pe}_T \lesssim 1$). This is an analogous result as for isotropic elements.

The remainder of the paper is organised as follows. The model problem is introduced in Section 2. The notation and some auxiliary results are presented in Section 3. The interpolation results of Section 3.3 deserve particular attention since they describe the alignment of anisotropic mesh and function. Section 4 then presents *residual error estimation* while Section 5 is devoted to error estimation via *local problems*. The numerical experiments of Section 6 confirm the theoretical predictions but also shed light on limitations of the estimators.

2 Model problem and its discretization

Assume that $\Omega \subset \mathbb{R}^d, d = 2, 3$, is a bounded polyhedral domain with Lipschitz boundary $\partial\Omega = \Gamma_{\mathrm{D}} \cup \Gamma_{\mathrm{N}}$. In our exposition we will only address the more technical three dimensional case; the 2D analogues can be derived easily.

For a bounded domain $\omega \subset \mathbb{R}^d, d = 2, 3$, we denote by $L^2(\omega)$ the usual Lebesgue space equipped with the norm $\| \cdot \|_\omega$ and the scalar product $(\cdot, \cdot)_\omega$. Similarly introduce the standard space $L^\infty(\omega)$ with norm $\| \cdot \|_{\infty,\omega}$, and let $H^1(\omega)$ be the usual Sobolev space, cf. [Ada75]. For the whole domain $\omega = \Omega$ the index of the norms will be omitted.

We are interested in the convection dominated case of (1) and assume

(A1) $\underline{b} \in W^{1,\infty}(\Omega)^d,\ c \in L^\infty(\Omega)$

(A2) There exists a positive constant c_0: $-\frac{1}{2}\nabla \cdot \underline{b} + c \geq c_0 > 0$

(A3) $\underline{b} \cdot n \geq 0$ on Γ_{N}.

Next, define an *energy norm* which is closely related to the differential equation by

$$|||v|||_\omega^2 := \varepsilon \|\nabla v\|_\omega^2 + c_0 \|v\|_\omega^2 \qquad . \tag{2}$$

Let $H_o^1(\Omega)$ be the standard Sobolev space of functions of $H^1(\Omega)$ with vanishing trace on Γ_{D}. The variational formulation corresponding to (1) becomes:

$$\text{Find } u \in H_o^1(\Omega): \qquad B(u, v) = \langle F, v \rangle \qquad \forall\, v \in H_o^1(\Omega) \tag{3}$$

with
$$\begin{aligned} B(u, v) &:= \varepsilon(\nabla u, \nabla v) + (\underline{b} \cdot \nabla u, v) + (cu, v) \\ \langle F, v \rangle &:= (f, v) + (g, v)_{\Gamma_{\mathrm{N}}} \qquad . \end{aligned}$$

Thanks to assumptions (A1)–(A3) the bilinear form $B(\cdot, \cdot)$ satisfies

$$B(v, v) \geq |||v|||^2 \qquad \forall v \in H_o^1(\Omega) \tag{4}$$

$$B(v, w)|_\omega \leq |||v|||_\omega \cdot \left(\max\{1, c_0^{-1}\|c\|_{\infty,\omega}\}\, |||w|||_\omega + \varepsilon^{-1/2}\|\underline{b}\|_{\infty,\omega}\|w\|_\omega\right) \tag{5}$$

for all $v, w \in H^1(\omega)$. The Lax Milgram lemma ensures existence and uniqueness of the weak solution u of (3).

Next, introduce a family $\mathcal{F} = \{\mathcal{T}\}$ of triangulations $\mathcal{T}$ of Ω that consist of tetrahedra. We assume an admissible triangulation in the sense of [Cia78]. Let $V_{o,h} \subset H_o^1(\Omega)$ be the space of continuous, piecewise linear functions over $\mathcal{T}$ that vanish on Γ_{D}.

The variational problem (3) is now discretized with the *streamline upwind Petrov Galerkin* scheme (SUPG):

$$\text{Find } u_h \in V_{o,h}: \qquad B_\delta(u_h, v_h) = \langle F_\delta, v_h \rangle \qquad \forall\, v \in V_{o,h} \tag{6}$$

with
$$\begin{aligned} B_\delta(u_h, v_h) &:= B(u_h, v_h) + \sum_{T \in \mathcal{T}} \delta_T \left(-\varepsilon \Delta u_h + \underline{b} \cdot \nabla u_h + cu_h, \underline{b} \cdot \nabla v_h\right)_T \\ \langle F_\delta, v_h \rangle &:= \langle F, v_h \rangle + \sum_{T \in \mathcal{T}} \delta_T \left(f, \underline{b} \cdot \nabla v_h\right)_T \qquad . \end{aligned}$$

When the real stabilization parameters δ_T vanish for all elements T then (6) coincides with the standard Galerkin discretization. In the singularly perturbed case ($\varepsilon \ll 1$) this discretization is unsuitable since it suffers from severe instabilities. Then the stabilized SUPG discretization (corresponding to $\delta_T > 0$) is more appropriate.

The discrete solution u_h exists and is unique if the stabilization parameters δ_T are sufficiently small. Following [RST96, Section III.3.2.1], one can show that

$$0 \leq \delta_T \leq \frac{1}{2} \min\{c_0 \|c\|_{\infty,T}^{-2} \,,\; h_{min,T}^2 \, \varepsilon^{-1} \mu^{-2}\}$$

is sufficient (see also [HL98, Section 2.2]). Here $h_{min,T}$ is the minimal length of an element T, see Section 3.1 below for a precise definition. The constant μ is such that the inverse inequality

$$\| \operatorname{div} \nabla v_h \|_T \leq \mu h_{min,T}^{-1} \| \nabla v_h \|_T$$

holds for all $v_h \in V_{o,h}$. For the case of piecewise linear functions in $V_{o,h}$ as considered here, this simplifies to $\mu = 0$ and (after some refined calculation) to $0 \leq \delta_T \leq c_0 \|c\|_{\infty,T}^{-2}$. In the sequel we always assume

$$\delta_T \lesssim h_{min,T} \|\underline{b}\|_{\infty,T}^{-1} \qquad \forall\, T \in \mathcal{T}$$

This demand is met for all kinds of stabilisation employed in our work, cf. the numerical experiments and Section 6.4 in particular. Furthermore it is advantageous to define a so–called *local mesh Peclet number* by

$$\mathrm{Pe}_T := \frac{\|\underline{b}\|_{\infty,T} h_{min,T}}{2\varepsilon} \qquad ,$$

cf. [HL98, Section 2.4] or the isotropic counterpart [RST96, Section III.3.2.1]. This mesh Peclet number relates the ratio of local convection and diffusion to the minimal local mesh size.

3 Notation and auxiliary results

Let $\mathbb{P}^k(\omega)$ be the space of polynomials of order k at most over some domain ω. To avoid excessive use of constants, we employ the shorthand notation $x \lesssim y$ and $x \sim y$ as abbreviation for $x \leq c \cdot y$ or $c_1 x \leq y \leq c_2 x$, respectively (with positive constants independent of x, y and $\varepsilon, \mathcal{T}$).

3.1 Notation

Tetrahedron: Denote the four vertices of an arbitrary tetrahedron $T \in \mathcal{T}$ by $P_0, \ldots, P_3$ such that P_0P_1 is the longest edge of T, $\mathrm{meas}_2(\triangle P_0P_1P_2) \geq \mathrm{meas}_2(\triangle P_0P_1P_3)$, and that $\mathrm{meas}_1(P_1P_2) \geq \mathrm{meas}_1(P_0P_2)$. Introduce three mutually orthogonal vectors $\mathbf{p}_{i,T}$ of length $h_{i,T} := |\mathbf{p}_{i,T}|$ according to Figure 1. Then $h_{1,T} > h_{2,T} \geq h_{3,T}$. Set

$$h_{min,T} := h_{3,T}$$

and define the matrix

$$C_T := (\mathbf{p}_{1,T}, \mathbf{p}_{2,T}, \mathbf{p}_{3,T}) \in \mathbb{R}^{3\times 3} \quad . \tag{7}$$

Furthermore introduce the scaling factor α_T that will be used frequently,

$$\alpha_T := \min\{c_0^{-1/2}, \varepsilon^{-1/2} \cdot h_{min,T}\} \quad . \tag{8}$$

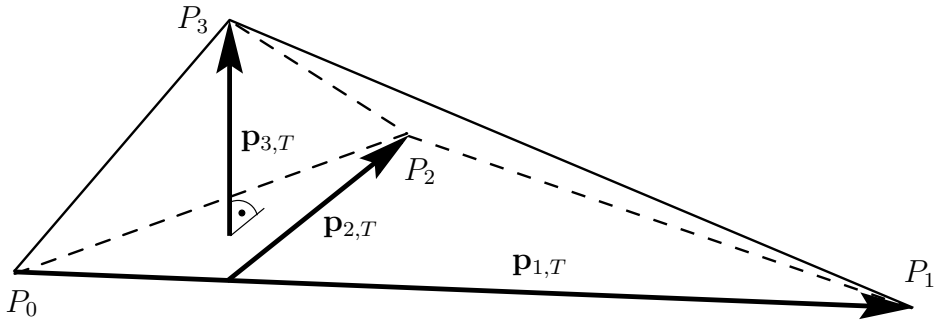

Figure 1: Notation of tetrahedron T

We denote tetrahedra by T, T' or T_i, and faces thereof by E. The length of the *height* over a face E is given by

$$h_{E,T} := 3\,\mathrm{meas}_3(T)/\mathrm{meas}_2(E) \quad .$$

For a face E, let ω_E be the domain formed by both neighbouring tetrahedra, with obvious modifications for a boundary face. For a tetrahedron T, define the domain ω_T that consists of T and its (generically four) face neighbouring tetrahedra. For convenience, define the mesh Peclet number on this domain by

$$\mathrm{Pe}_{\omega_T} := \max_{T'\subset\omega_T} \mathrm{Pe}_{T'} \quad . \tag{9}$$

Mesh requirements: In addition to the standard admissibility conditions of the mesh [Cia78, Chapter 2] we require two further assumptions.

1. The number of tetrahedra containing a node x_j is bounded uniformly.
2. The dimensions of adjacent tetrahedra must not change rapidly, i.e.

$$h_{i,T'} \sim h_{i,T} \qquad \forall\, T, T' \text{ with } T \cap T' \neq \emptyset\,,\ i = 1\ldots 3 \quad .$$

For notational simplicity it is convenient to employ also *face based* quantities (instead of *element based* terms as e.g. $h_{min,T}$). Therefore we consider an interior face $E = T_1 \cap T_2$ and define

$$h_E := (h_{E,T_1} + h_{E,T_2})/2, \qquad h_{min,E} := (h_{min,T_1} + h_{min,T_2})/2, \qquad \alpha_E := (\alpha_{T_1} + \alpha_{T_2})/2 \quad .$$

Consequently these terms are no longer related to T_1 or T_2 but to E. Because of the previous mesh requirements they satisfy $h_E \sim h_{E,T_i}$, $h_{min,E} \sim h_{min,T_i}$ and $\alpha_E \sim \alpha_{T_i}$. For a boundary face $E \subset \partial T \cap \partial\Omega$ define similarly $h_E := h_{E,T}$, $h_{min,E} := h_{min,T}$ and $\alpha_E := \alpha_T$.

Squeezed tetrahedron $T_{E,\gamma}$: The squeezed tetrahedra have proven to be useful in previous work [Ver98a, Kun01b, Kun01c]. Here we repeat the main results.

Start with a tetrahedron T and an arbitrary face E thereof. Denote the vertices of T such that $E = Q_1Q_2Q_3$ and $T = PQ_1Q_2Q_3$, and let S_E be the midpoint of the face E, cf. Figure 2.

For $\gamma \in (0, 1]$ being a real parameter, construct the point P_γ on the line S_EP such that $|\vec{S_EP_\gamma}| = \gamma \cdot |\vec{S_EP}|$. The *squeezed tetrahedron* is now defined as $T_{E,\gamma} = P_\gamma Q_1Q_2Q_3$.

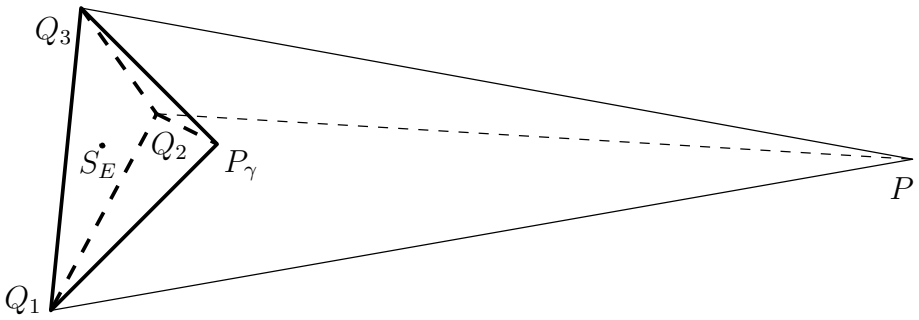

Figure 2: Tetrahedra $T = PQ_1Q_2Q_3$ and $T_{E,\gamma} = P_\gamma Q_1Q_2Q_3$

Finally consider the affine linear mapping $F_{T,E,\gamma}$ that maps the unit tetrahedron to the squeezed tetrahedron $T_{E,\gamma}$. In the next section we require a bound of the inverse transformation matrix which has been proven in [Kun01b],

$$\|F^{-1}_{T,E,\gamma}\|_{\mathbb{R}^{3\times3}} \lesssim \min\{\gamma \cdot h_{E,T}\ ,\ h_{min,T}\}^{-1} \quad . \tag{10}$$

3.2 Bubble functions

Bubble functions are an approved tool to obtain lower error bounds. Here we recapitulate some standard definitions and results (cf. [Ver96]) before we present refined face bubble functions.

Denote the barycentric coordinates of an arbitrary tetrahedron T by $\lambda_{T,1}, \cdots, \lambda_{T,4}$. The *element bubble function* is defined by

$$b_T := 4^4 \cdot \lambda_{T,1} \cdot \lambda_{T,2} \cdot \lambda_{T,3} \cdot \lambda_{T,4} \in \mathbb{P}^4(T) \qquad \text{on } T \quad . \tag{11}$$

Consider next an (interior) face $E = T_1 \cap T_2$. Enumerate the vertices of T_1 and T_2 such that the vertices of E are numbered first, and define the *standard face bubble function* $b_E \in C^0(\omega_E)$ by

$$b_E|_{T_i} := 3^3 \cdot \lambda_{T_i,1} \cdot \lambda_{T_i,2} \cdot \lambda_{T_i,3} \qquad \text{on } T_i,\ i = 1, 2 \quad .$$

For boundary faces modify b_E appropriately. The element and face bubble functions are extended by zero outside their original domain of definition.

For conceptual clarity we also introduce an extension operator $F_{ext} : \mathbb{P}^0(E) \to \mathbb{P}^0(\omega_E)$ that maps a constant function over a face E to the same constant function on ω_E.

Lemma 1 (Equivalences for bubble functions) *Let $\varphi_T \in \mathbb{P}^0(T)$ and $\varphi_E \in \mathbb{P}^0(E)$. Then*

$$\|b_T^{1/2} \cdot \varphi_T\|_T \sim \|\varphi_T\|_T \tag{12}$$
$$\|b_E^{1/2} \cdot \varphi_E\|_E \sim \|\varphi_E\|_E \tag{13}$$

Proof: Both equivalences are easily obtained by standard scaling techniques. ∎

For the analysis of singularly perturbed reaction/convection–diffusion problems one can favourably employ modified face bubble functions that originate from [Ver98b] and [Kun01b]. Here we repeat the definition and main results; for more details see also [Kun01c].

Consider a face E and its two neighbouring tetrahedra T_1 and T_2. For a real number $\gamma \in (0, 1]$ construct both squeezed tetrahedra $T_{i,E,\gamma}$, cf. Figure 2. The *squeezed face bubble function* $b_{E,\gamma}$ is defined as the standard face bubble function for the *squeezed tetrahedra* $T_{1,E,\gamma}$ and $T_{2,E,\gamma}$. Outside of $T_{1,E,\gamma} \cup T_{2,E,\gamma}$ the function $b_{E,\gamma}$ is set to zero. Figure 3 depicts this definition for the 2D analogue.

Later on, the following inverse inequalities will be required.

Lemma 2 (Inverse inequalities) *Let E be an arbitrary face of T. Assume $\varphi_T \in \mathbb{P}^0(T)$, $\varphi_E \in \mathbb{P}^0(E)$, and let $\gamma \in (0, 1]$ be arbitrary. Then*

$$\|b_{E,\gamma} \cdot F_{ext}(\varphi_E)\|_T \lesssim \gamma^{1/2} \cdot h_{E,T}^{1/2} \cdot \|\varphi_E\|_E \tag{14}$$
$$\|\nabla(b_{E,\gamma} \cdot F_{ext}(\varphi_E))\|_T \lesssim \gamma^{1/2} \cdot h_{E,T}^{1/2} \cdot \min\{\gamma \cdot h_{E,T}\ ,\ h_{min,T}\}^{-1} \cdot \|\varphi_E\|_E \tag{15}$$
$$|||b_{E,\gamma} \cdot F_{ext}(\varphi_E)|||_T \lesssim \gamma^{1/2} \cdot h_{E,T}^{1/2} \cdot \left(c_0^{1/2} + \varepsilon^{1/2} \min\{\gamma \cdot h_{E,T}\ ,\ h_{min,T}\}^{-1}\right) \cdot \|\varphi_E\|_E \tag{16}$$
$$|||b_T \cdot \varphi_T|||_T \lesssim \alpha_T^{-1} \|\varphi_T\|_T. \tag{17}$$

Proof: Inequalities (14) and (15) require a careful analysis of the underlying geometrical properties of the squeezed tetrahedron, see e.g. the bound (10). The proof of both relations is given in detail in [Kun01b, Lemma 3.7]. A combination provides directly the corresponding bound (16) in the energy norm.

Finally, by standard scaling techniques one concludes $\|\nabla(b_T \cdot \varphi_T)\|_T \lesssim h_{min,T}^{-1} \cdot \|\varphi_T\|_T$ for arbitrary $\varphi_T \in \mathbb{P}^0(T)$. Together with $\|b_T \cdot \varphi_T\|_T \leq \|\varphi_T\|_T$ and the definition (8) of α_T one infers (17). ∎

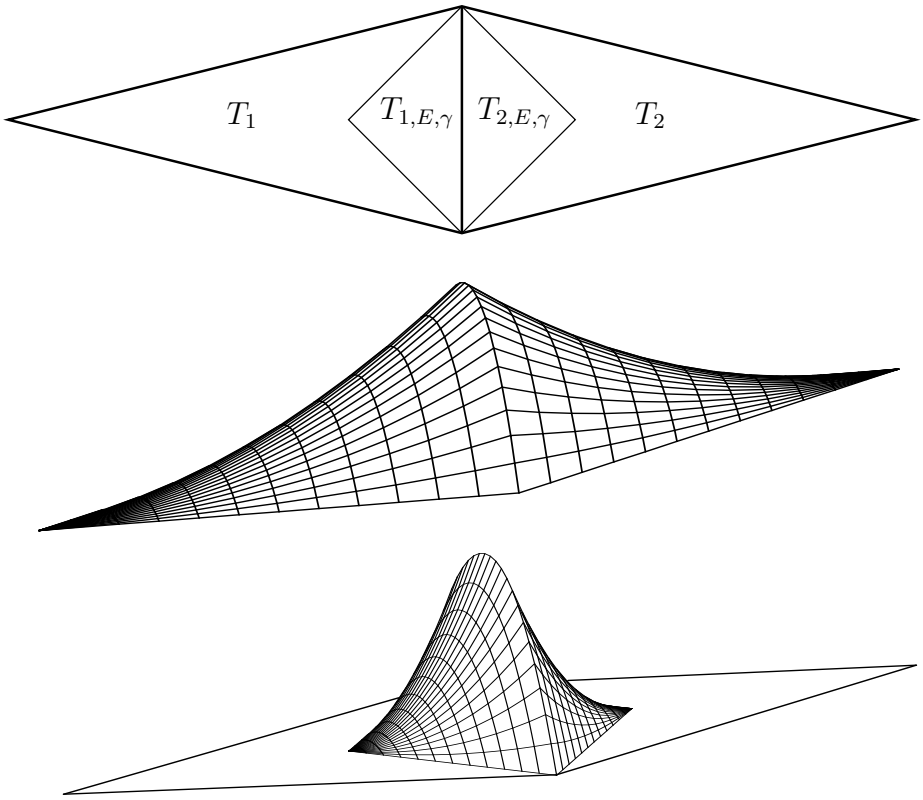

Figure 3: Top: ω_E and squeezed triangles $T_{i,E,\gamma}$ (2D case)
Middle: standard face bubble function b_E
Bottom: squeezed face bubble function $b_{E,\gamma}$

3.3 Interpolation results

Within the last decade research has been increasingly focusing on error estimators for anisotropic meshes. Primarily one is interested in reliable and efficient *a posteriori* error estimators, i.e. upper and lower error bounds should hold. Unfortunately, up to now reliability *and* efficiency at the same time can be guaranteed only if the anisotropy of the mesh is sufficiently aligned with the anisotropic function. For example, in [Sie96] the analysis is restricted to a certain set of treatable anisotropic functions. In [Kun99, Kun00, Kun01b] a so–called *matching function* $m_1(v, \mathcal{T})$ is introduced which measures the alignment of an anisotropic function v and an anisotropic mesh $\mathcal{T}$. Lastly, in Dobrowolski/Gräf/Pflaum [DGP99] a saturation assumption is necessary that implies a similar correspondence.

Here we follow the approach of Kunert and present the *matching function* [Kun99, Kun00]. This matching function plays an important role in the anisotropic interpolation estimates and, subsequently, in the upper error bounds (cf. Lemma 3 and Theorems 4 and 7 below).

Definition 1 (Matching function) *Let $v \in H^1(\Omega)$, and $\mathcal{T} \in \mathcal{F}$ be a triangulation of Ω. Define the* matching function *$m_1 : H^1(\Omega) \times \mathcal{F} \mapsto \mathbb{R}$ by*

$$m_1(v,\mathcal{T}) \;:=\; \Big(\sum_{T\in\mathcal{T}} h_{min,T}^{-2} \cdot \|C_T^T \nabla v\|_T^2 \Big)^{1/2} \Big/ \, \|\nabla v\| \qquad , \tag{18}$$

with the matrix $C_T \in \mathbb{R}^{3\times 3}$ given by (7).

Further discussion can be found in the aforementioned literature. Here few remarks shall give some impressions of the behaviour of the matching function.

First, with the temporary notation $h_{max,T} := h_{1,T}$, one concludes

$$1 \;\le\; m_1(v,\mathcal{T}) \lesssim \max_{T\in\mathcal{T}} h_{max,T}/h_{min,T} \qquad .$$

This upper bound on m_1 is practically useless. It confirms, however, that $m_1 \sim 1$ on isotropic meshes, and the matching function merges there with other constants. Hence (18) can be regarded as a natural extension of the theory for isotropic meshes.

On anisotropic meshes that are *well aligned* with an anisotropic function v one also obtains $m_1(v,\mathcal{T}) \sim 1$; in practical experiments m_1 mostly ranges from 1.5 to 4. If the anisotropic mesh is *not aligned* with an anisotropic function v then the matching function can be arbitrarily large. Consequently the error can be extremely overestimated, i.e. the error estimator becomes practically useless [Kun01a, Section 4.2].

Next we state anisotropic interpolation results which form an indispensable ingredient for the analysis of the residual error estimator. Since the usual Lagrange interpolant is not defined for functions $v \in H^1(\Omega)$, we resort to to Clément interpolation operator I_{Cl}, cf. also [Clé75]. In [Kun00] the interpolation estimates have been extended to anisotropic tetrahedral meshes. The results have been adapted to suit the analysis of a singularly perturbed reaction–diffusion problem in [Kun01b]. Note that all anisotropic interpolation estimates contain the aforementioned matching function.

Here we repeat the interpolation estimates obtained in [Kun01b].

Lemma 3 (Clément interpolation) *Let $v \in H_o^1(\Omega)$ and α_T given by (8). The Clément interpolation operator $I_{\mathrm{Cl}} : H_o^1(\Omega) \mapsto V_{o,h}$ satisfies the inequalities below:*

$$|||I_{\mathrm{Cl}} v||| \;\lesssim\; m_1(v,\mathcal{T}) \cdot |||v||| \tag{19}$$

$$\sum_{T\in\mathcal{T}} \alpha_T^{-2} \cdot \|v - I_{\mathrm{Cl}} v\|_T^2 \;\lesssim\; m_1(v,\mathcal{T})^2 \cdot |||v|||^2 \tag{20}$$

$$\varepsilon^{1/2} \sum_{E\subset\Omega\setminus\Gamma_{\mathrm{D}}} \alpha_E^{-1} \cdot \|v - I_{\mathrm{Cl}} v\|_E^2 \;\lesssim\; m_1(v,\mathcal{T})^2 \cdot |||v|||^2 \qquad . \tag{21}$$

Proof: The stability estimate (19) follows from the inequalities

$$\begin{aligned} \|I_{\mathrm{Cl}} v\| &\lesssim \|v\| \\ \|\nabla I_{\mathrm{Cl}} v\| &\lesssim m_1(v,\mathcal{T}) \cdot \|\nabla v\| \end{aligned}$$

which can be proven exactly as in [Kun00, Section 3]. The last two inequalities are proven in [Kun01b, Lemma 3.11]. ∎

4 Residual error estimation

Error bounds can be obtained by measuring and scaling the residuals, cf. the textbooks [AO00, Ver96]. The general approach here is similar, and it follows the analysis for the convection–diffusion problem on isotropic elements [Ver98a]. All the details here are of course tailored to take the anisotropy of the elements into account. More precisely, the upper error bound is based on specific anisotropic interpolation estimates while the lower error bound relies on (adapted) bubble functions and corresponding inverse inequalities. It is noteworthy that we can utilize most of the techniques and ingredients that were derived to analyse *reaction–diffusion* problems (cf. [Kun01b]).

In Section 4.1 we propose and analyse error bounds for a piecewise *linear* finite element solution u_h and piecewise *constant* approximate residuals. Section 4.2 is devoted to higher order approximations.

4.1 Error estimation using constant approximate residuals

We start with the definition of the (exact and approximate) residuals, and of the error estimator.

Exact residuals: For an element T and a face E define the *exact element residual* R_T and the *exact face residual* R_E as follows:

$$\begin{aligned} R_T &:= f - (-\varepsilon \Delta u_h + \underline{b} \cdot \nabla u_h + c u_h) \qquad \text{on } T, \\ R_E(x) &:= \begin{cases} \varepsilon \cdot \lim\limits_{t \to +0} \left[\partial_{n_E} u_h(x + t n_E) - \partial_{n_E} u_h(x - t n_E) \right] & \text{if } E \subset \Omega \setminus \Gamma \\ g - \varepsilon \cdot \partial_n u_h & \text{if } E \subset \Gamma_{\mathrm{N}} \\ 0 & \text{if } E \subset \Gamma_{\mathrm{D}} \end{cases} . \end{aligned}$$

Here $n_E \perp E$ is any of the two unitary normal vectors whereas $n \perp E \subset \Gamma_{\mathrm{N}}$ denotes the outer unitary normal vector.

Approximate residuals: Parts of the theory require residual terms from a finite dimensional space. Therefore we utilize an approximation operator $\mathcal{P}$ that approximates the element residual and the face residual by piecewise *constant* values, respectively. By these means we define the *(approximate) element residual* r_T and the *(approximate) face residual* r_E:

$$\begin{aligned} r_T &:= \mathcal{P}(R_T) \in \mathbb{P}^0(T) \qquad \forall\, T \in \mathcal{T} \\ r_E &:= \mathcal{P}(R_E) \in \mathbb{P}^0(E) \qquad \forall\, E \qquad . \end{aligned}$$

Since the finite element solution u_h is linear, the exact face residual R_E is already constant for interior faces or Dirichlet faces. Hence it is natural to demand

$$r_E = R_E \qquad \forall\, E \subset \Omega \setminus \Gamma_{\mathrm{N}} \quad ,$$

i.e. the face residual is approximated only for Neumann boundary faces.

Note also that formally the approximations can be chosen arbitrarily. In order to obtain tight results, the approximation error should nevertheless be small (cf. the results below).

Definition 2 (Residual error estimator) *For a tetrahedron T, the* residual error estimator $\eta_{\mathrm{R},T}$ *and the* approximation term ζ_T *are defined by*

$$\begin{aligned} \eta_{\mathrm{R},T}^2 &:= \alpha_T^2 \cdot \|r_T\|_T^2 + \varepsilon^{-1/2} \cdot \alpha_T \cdot \sum_{E \subset \partial T \setminus \Gamma_{\mathrm{D}}} \|r_E\|_E^2 \\ \zeta_T^2 &:= \alpha_T^2 \cdot \|r_T - R_T\|_{\omega_T}^2 + \varepsilon^{-1/2} \cdot \alpha_T \cdot \sum_{E \subset \partial T \cap \Gamma_{\mathrm{N}}} \|r_E - R_E\|_E^2 \quad , \end{aligned}$$

where the scaling factor α_T is given by (8). Furthermore define the corresponding global *expressions by*

$$\eta_{\mathrm{R}}^2 := \sum_{T \in \mathcal{T}} \eta_{\mathrm{R},T}^2 \qquad \textit{and} \qquad \zeta^2 := \sum_{T \in \mathcal{T}} \zeta_T^2 \quad .$$

Now we are ready to state the error bounds. The upper error bound involves the alignment of the anisotropic mesh and the anisotropic solution. Thus *reliable* error estimation is achieved for suitable meshes. The lower error bound contains an additional and potentially large factor that is related to the local mesh Peclet number. Hence one can guarantee efficiency of the error estimator only for small Peclet numbers $\mathrm{Pe}_T \lesssim 1$. This result is analogous to the isotropic counterpart (but different to e.g. the Poisson problem or the reaction–diffusion problem). For more details see also Remark 2 and the numerical experiments of Section 6.

The main theoretical result is presented next.

Theorem 4 (Residual error estimation) *The error is bounded locally from below for all $T \in \mathcal{T}$ by*

$$\eta_{\mathrm{R},T} \lesssim |||u - u_h|||_{\omega_T} \cdot \left(\max\{1, c_0^{-1} \|c\|_{\infty,\omega_T}\} + \varepsilon^{-1/2} \alpha_T \|\underline{b}\|_{\infty,\omega_T} \right) + \zeta_T \quad . \tag{22}$$

Recalling Pe_{ω_T} *from (9), this lower bound can be rewritten in the slightly weaker form*

$$\eta_{\mathrm{R},T} \lesssim |||u - u_h|||_{\omega_T} \cdot \left(\max\{1, c_0^{-1} \|c\|_{\infty,\omega_T}\} + \mathrm{Pe}_{\omega_T} \right) + \zeta_T \quad . \tag{23}$$

Assume further that the stabilization parameters satisfy $\delta_T \lesssim h_{min,T} / \|\underline{b}\|_{\infty,T}$. Then the error is bounded globally from above by

$$|||u - u_h||| \lesssim m_1(u - u_h, \mathcal{T}) \cdot \left[\eta_{\mathrm{R}}^2 + \zeta^2 \right]^{1/2} \quad . \tag{24}$$

Proof: The proof follows the lines of [Ver98a], with appropriate modifications for anisotropic elements. We start with a basic error equation. Element–wise integration by parts yields for all $w \in H_o^1(\Omega)$

$$B(u - u_h, w) = \sum_{T \in \mathcal{T}} (R_T, w)_T + \sum_{E \subset \Omega \setminus \Gamma_{\mathrm{D}}} (R_E, w)_E \quad . \tag{25}$$

In order to derive the lower error bound (22), we have to bound $\|r_T\|_T$ and $\|r_E\|_E$. To this end insert $w_T := b_T \cdot r_T$ into (25) and conclude

$$(r_T, w_T)_T = B(u - u_h, w_T) + (r_T - R_T, w_T)_T \quad .$$

The bilinear form is bounded using (5). With the inverse inequality (17) and the obvious relation $\|w_T\|_T \leq \|r_T\|_T$ this yields

$$\begin{aligned} B(u-u_h, w_T) &\leq |||u-u_h|||_T \left(\max\{1, c_0^{-1}\|c\|_{\infty,T}\} \, |||w_T|||_T + \varepsilon^{-1/2}\|\underline{b}\|_{\infty,T}\|w_T\|_T\right) \\ &\overset{(17)}{\lesssim} |||u-u_h|||_T \cdot \|r_T\|_T \cdot \left(\max\{1, c_0^{-1}\|c\|_{\infty,T}\}\alpha_T^{-1} + \varepsilon^{-1/2}\|\underline{b}\|_{\infty,T}\right) \quad . \end{aligned}$$

Using $(r_T - R_T, w_T)_T \leq \|r_T - R_T\|_T \, \|r_T\|_T$ and $(r_T, w_T)_T \sim \|r_T\|_T^2$ from (12) one obtains

$$\alpha_T\|r_T\|_T \lesssim |||u-u_h|||_T \left(\max\{1, c_0^{-1}\|c\|_{\infty,T}\} + \varepsilon^{-1/2}\alpha_T\|\underline{b}\|_{\infty,T}\right) + \alpha_T\|r_T - R_T\|_T \quad .$$

Next the norm of the face residuals is to be bounded. Let us start with an interior face $E = T_1 \cap T_2$ and recall $r_E = R_E \in \mathbb{P}^0(E)$ (i.e. the approximate residual is exact). Set

$$w_E := b_{E,\gamma_E} \cdot F_{ext}(r_E) \quad .$$

Here the parameter γ_E is chosen to be

$$\gamma_E := \min\left\{1 \, , \, \frac{h_{min,E}}{h_E} \, , \, \frac{\varepsilon^{1/2}}{c_0^{1/2} h_E}\right\} \tag{26}$$

which implies $\gamma_E \sim \varepsilon^{1/2}\alpha_E h_E^{-1} \sim \varepsilon^{1/2}\alpha_{T_i} h_E^{-1}$. Insert w_E in equation (25) and infer

$$(r_E, w_E)_E = B(u-u_h, w_E) - \sum_{i=1}^{2}(r_{T_i}, w_E)_{T_i} + \sum_{i=1}^{2}(r_{T_i} - R_{T_i}, w_E)_{T_i} \quad .$$

The L^2 scalar products are bounded using the Cauchy Schwarz inequality, several inverse inequalities and the specific value of γ_E.

$$\begin{aligned} (r_E, w_E)_E &= (r_E, b_E r_E)_E \overset{(13)}{\sim} \|r_E\|_E^2 \\ \|w_E\|_{T_i} &\overset{(14)}{\lesssim} \varepsilon^{1/4}\alpha_{T_i}^{1/2}\|r_E\|_E \\ |||w_E|||_{T_i} &\overset{(16)}{\lesssim} \varepsilon^{1/4}\alpha_{T_i}^{-1/2}\|r_E\|_E \quad . \end{aligned}$$

Applying these inequalities and relation (5) to $B(u-u_h, w_E)$ results in

$$\begin{aligned} B(u-u_h, w_E) &\overset{(5)}{\lesssim} |||u-u_h|||_{\omega_E} \cdot \left(\max\{1, c_0^{-1}\|c\|_{\infty,\omega_E}\} \, |||w_E|||_{\omega_E} + \varepsilon^{-1/2}\|\underline{b}\|_{\infty,\omega_E}\|w_E\|_{\omega_E}\right) \\ &\lesssim |||u-u_h|||_{\omega_E} \cdot \|r_E\|_E \left(\max\{1, c_0^{-1}\|c\|_{\infty,\omega_E}\} \, \varepsilon^{1/4}\alpha_E^{-1/2} + \varepsilon^{-1/4}\alpha_E^{1/2}\|\underline{b}\|_{\infty,\omega_E}\right). \end{aligned}$$

Combining all these inequalities and utilizing the previous bound of $\|r_T\|_T$ gives

$$\begin{aligned} \varepsilon^{-1/4}\alpha_E^{1/2}\|r_E\|_E \lesssim{}& |||u-u_h|||_{\omega_E} \left(\max\{1, c_0^{-1}\|c\|_{\infty,\omega_E}\} + \varepsilon^{-1/2}\alpha_E\|\underline{b}\|_{\infty,\omega_E}\right) \\ &+ \alpha_E \sum_{i=1}^{2}\|r_{T_i} - R_{T_i}\|_{T_i} \quad . \end{aligned}$$

For a Neumann boundary face $E \subset \Gamma_N$ of an element T one proceeds similarly to conclude

$$\begin{aligned}\varepsilon^{-1/4}\alpha_E^{1/2}\|r_E\|_E \;\lesssim\; &|||u-u_h|||_T\left(\max\{1,c_0^{-1}\|c\|_{\infty,T}\}+\varepsilon^{-1/2}\alpha_E\|\underline{b}\|_{\infty,T}\right)\\ &+\alpha_E\|r_T-R_T\|_T+\varepsilon^{-1/4}\alpha_E^{1/2}\|r_E-R_E\|_E \quad .\end{aligned}$$

Next recall that $\alpha_E \sim \alpha_T$ for $E \subset \partial T$. All inequalities together then prove the lower error bound (22). Finally note that the term $\varepsilon^{-1/2}\alpha_T\|\underline{b}\|_{\infty,\omega_T}$ of (22) can be bounded by the local mesh Peclet number,

$$\varepsilon^{-1/2}\alpha_T\|\underline{b}\|_{\infty,\omega_T} \lesssim \max_{T'\subset\omega_T} \mathrm{Pe}_{T'} \;=\; \mathrm{Pe}_{\omega_T}$$

which proves the slightly weaker bound (23).

In order to prove the upper error bound (24), we employ (4) and obtain

$$|||u-u_h||| \overset{(4)}{\leq} \frac{B(u-u_h,u-u_h)}{|||u-u_h|||} = \frac{B(u-u_h,v)}{|||v|||} \quad ,$$

with $v := u - u_h$. The numerator is now decomposed with the help of the Clément interpolation operator I_{Cl},

$$B(u-u_h,v) = B(u-u_h,v-I_{\mathrm{Cl}}v) + B(u-u_h,I_{\mathrm{Cl}}v) \quad .$$

The middle term is treated via (25) and results in

$$B(u-u_h,v-I_{\mathrm{Cl}}v) = \sum_{T\in\mathcal{T}}(R_T,v-I_{\mathrm{Cl}}v)_T + \sum_{E\subset\Omega\setminus\Gamma_D}(R_E,v-I_{\mathrm{Cl}}v)_E \quad .$$

The Cauchy Schwarz inequality and the interpolation results of Lemma 3 yield

$$\begin{aligned}\sum_{T\in\mathcal{T}}(R_T,v-I_{\mathrm{Cl}}v)_T \;&\leq\; \left(\sum_{T\in\mathcal{T}}\alpha_T^2\|R_T\|_T^2\right)^{1/2}\cdot\left(\sum_{T\in\mathcal{T}}\alpha_T^{-2}\|v-I_{\mathrm{Cl}}v\|_T^2\right)^{1/2}\\ &\overset{(20)}{\lesssim}\; \left(\sum_{T\in\mathcal{T}}\alpha_T^2\|R_T\|_T^2\right)^{1/2}\cdot m_1(v,\mathcal{T})\cdot|||v|||\\ \sum_{E\subset\Omega\setminus\Gamma_D}(R_E,v-I_{\mathrm{Cl}}v)_E \;&\leq\; \left(\sum_{E\subset\Omega\setminus\Gamma_D}\varepsilon^{-1/2}\alpha_E\|R_E\|_E^2\right)^{1/2}\cdot\left(\sum_{E\subset\Omega\setminus\Gamma_D}\varepsilon^{1/2}\alpha_E^{-1}\|v-I_{\mathrm{Cl}}v\|_E^2\right)^{1/2}\\ &\overset{(21)}{\lesssim}\; \left(\sum_{E\subset\Omega\setminus\Gamma_D}\varepsilon^{-1/2}\alpha_E\|R_E\|_E^2\right)^{1/2}\cdot m_1(v,\mathcal{T})\cdot|||v||| \quad .\end{aligned}$$

Thus the term $B(u-u_h,v-I_{\mathrm{Cl}}v)$ can be bounded by

$$B(u-u_h,v-I_{\mathrm{Cl}}v) \;\lesssim\; \left(\sum_{T\in\mathcal{T}}\alpha_T^2\|R_T\|_T^2+\sum_{E\subset\Omega\setminus\Gamma_D}\varepsilon^{-1/2}\alpha_E\|R_E\|_E^2\right)^{1/2}\cdot m_1(v,\mathcal{T})\cdot|||v||| \quad .$$

Consider now the last term $B(u-u_h, I_{\mathrm{Cl}}v)$ of the decomposition from above. This term is due to the SUPG discretization and vanishes for the standard Galerkin method. For an arbitrary function $v_h \in V_{o,h}$, standard scaling arguments readily imply $\|\nabla v_h\|_T \lesssim h_{min,T}^{-1}\|v_h\|_T \leq h_{min,T}^{-1} c_0^{-1/2} \,|||v_h|||_T$. Together with the obvious bound $\|\nabla v_h\|_T \leq \varepsilon^{-1/2}\,|||v_h|||_T$ one concludes

$$\|\nabla v_h\|_T \;\lesssim\; \min\{h_{min,T}^{-1} c_0^{-1/2}, \varepsilon^{-1/2}\}\,|||v_h|||_T \;=\; h_{min,T}^{-1}\,\alpha_T\,|||v_h|||_T \qquad .$$

We now use the Galerkin orthogonality and recall that u_h is the solution of the SUPG discretization. Hence we can reformulate $B(u-u_h, I_{\mathrm{Cl}}v)$. With the previous inequality for $v_h := I_{\mathrm{Cl}}v$ and the stability estimate (19) of the Clément operator one obtains

$$\begin{aligned}
B(u-u_h, I_{\mathrm{Cl}}v) \quad &= \quad -\sum_{T\in\mathcal{T}} \delta_T\,(R_T, \underline{b}\cdot\nabla I_{\mathrm{Cl}}v)_T \\
&\leq \quad \sum_{T\in\mathcal{T}} \delta_T \|R_T\|_T \|\underline{b}\|_{\infty,T} \|\nabla I_{\mathrm{Cl}}v\|_T \\
&\lesssim \quad \sum_{T\in\mathcal{T}} \delta_T \|R_T\|_T \|\underline{b}\|_{\infty,T}\cdot h_{min,T}^{-1}\,\alpha_T\,|||I_{\mathrm{Cl}}v|||_T \\
&\overset{(19)}{\lesssim} \quad \left(\sum_{T\in\mathcal{T}} \delta_T^2 \|R_T\|_T^2 \|\underline{b}\|_{\infty,T}^2 \cdot h_{min,T}^{-2}\,\alpha_T^2\right)^{1/2} \cdot m_1(v,\mathcal{T})\cdot|||v||| \qquad .
\end{aligned}$$

The stabilisation parameter is assumed to satisfy $\delta_T \lesssim h_{min,T}/\|\underline{b}\|_{\infty,T}$ for all elements T. Then the last bound simplifies to

$$B(u-u_h, I_{\mathrm{Cl}}v) \;\lesssim\; \left(\sum_{T\in\mathcal{T}} \alpha_T^2 \|R_T\|_T^2\right)^{1/2} \cdot m_1(v,\mathcal{T})\cdot|||v||| \qquad .$$

Combine now all results and recall the abbreviation $v = u - u_h$ which gives

$$|||u-u_h||| \lesssim m_1(u-u_h,\mathcal{T})\cdot\left(\sum_{T\in\mathcal{T}} \alpha_T^2\|R_T\|_T^2 + \sum_{E\subset\Omega\setminus\Gamma_{\mathrm{D}}} \varepsilon^{-1/2}\alpha_E\|R_E\|_E^2\right)^{1/2} \qquad .$$

Finally the triangle inequalities for the (exact and approximate) residuals provide the upper error bound (24). ∎

Remark 1 It is possible to redefine the residual error estimator by

$$\begin{aligned}
\tilde{\eta}_{\mathrm{R},T}^2 \quad &:= \quad \alpha_T^2\cdot\|r_T\|_T^2 + \varepsilon^{-1/2}\cdot\alpha_T\cdot\sum_{E\subset\partial T\setminus\Gamma_{\mathrm{D}}} \frac{h_{min,E}}{h_E}\|r_E\|_E^2 \\
\tilde{\zeta}_T^2 \quad &:= \quad \alpha_T^2\cdot\|r_T - R_T\|_{\omega_T}^2 \;+\; \varepsilon^{-1/2}\cdot\alpha_T\cdot\sum_{E\subset\partial T\cap\Gamma_{\mathrm{N}}} \frac{h_{min,E}}{h_E}\|r_E - R_E\|_E^2 \qquad .
\end{aligned}$$

The only difference is the modified scaling of the face residual terms which implies

$$\tilde{\eta}_{\mathrm{R},T} \lesssim \eta_{\mathrm{R},T} \quad .$$

Consequently the same lower error bound (22) holds. A closer inspection of the Clément interpolation estimates (cf. [Kun99, Lemma 4.3]) reveals that a corresponding upper error bound (24) is also valid.

In the next section we will show the equivalence of the original residual error estimator $\eta_{\mathrm{R},T}$ with the local problem error estimator $\eta_{\mathrm{D},T}$. Such an equivalence could not be established for the modified residual estimator. □

Remark 2 When investigating error estimators, one often encounters the terms *reliable* and *efficient*. Up to approximation terms (or higher order terms), they commonly have the meaning

$$\begin{array}{rcrcl} \text{(global) Reliability} & \Leftrightarrow & |||u-u_h||| & \lesssim & \eta_{\mathrm{R}} \\ \text{(local) Efficiency} & \Leftrightarrow & \eta_{\mathrm{R},T} & \lesssim & |||u-u_h|||_{\omega_T} \end{array} \quad ,$$

i.e. they are closely related to (but not identical with) the upper and lower error bounds.

Let us compare these definitions with our main result of Theorem 4. We conclude that the error is *reliable* whenever the matching function is small, $m_1(u-u_h,\mathcal{T}) \sim 1$. This will be the case when the anisotropic mesh is well adapted to the anisotropic solution.

The *efficiency* requires a careful distinction for convection–diffusion problems. Recall the lower error bound (23),

$$\eta_{\mathrm{R},T} \lesssim |||u-u_h|||_{\omega_T} \cdot \left\{\max\{1, c_0^{-1}\|c\|_{\infty,\omega_T}\} + \mathrm{Pe}_{\omega_T}\right\} + \zeta_T \quad .$$

Assume for a moment $c_0 \sim \|c\|_{\infty,\omega_T}$, i.e. the behaviour of the factor on the right–hand side is essentially determined by the mesh Peclet numbers Pe_{ω_T}. Hence the above error bound implies efficiency only for small mesh Peclet numbers $\mathrm{Pe}_{\omega_T} \lesssim 1$. Such small Peclet numbers arise e.g. for (suitable) anisotropic elements in layer regions of exponential type (i.e. layers of width $\mathcal{O}(\varepsilon)$).

Conversely, for large mesh Peclet numbers the efficiency cannot be guaranteed since the error estimator $\eta_{\mathrm{R},T}$ may be large even when the error $|||u-u_h|||_{\omega_T}$ is small. Large Peclet numbers $\mathrm{Pe}_{\omega_T} \gg 1$ will usually arise for elements in coarse mesh regions or parabolic layer regions (i.e. layers of width $\mathcal{O}(\sqrt{\varepsilon})$). Numerical comparisons of [Joh00] indicate that the lacking efficiency is mainly a problem inside parabolic layers since the error is usually much larger there than in coarse mesh regions with a smooth solution.

Finally we remark that the partial loss of efficiency is not due to the anisotropic elements but to the dominating convection of the problem, cf. also [KS01, Ver98a]. □

4.2 Error estimation using higher order approximate residuals

The error estimator of section 4.1 is suitable for piecewise linear u_h and constant approximate residuals. Now we will discuss the changes that are necessary when *higher order approximate residuals* are used, or when *higher order ansatz functions* are employed to construct the finite element space $V_{o,h}$.

Let us start with higher order approximate residuals, i.e. r_T and r_E are no longer piecewise constant but instead $r_T \in \mathbb{P}^{k_1}(T)$ and $r_E \in \mathbb{P}^{k_2}(E)$. Then Lemma 1 remains valid although the inequality constants involved will depend on the polynomial degrees k_1 and k_2. Next the extension operator F_{ext} has to be modified such that it can be applied to functions from $\mathbb{P}^{k_2}(E)$. The standard choice as e.g. proposed by [Ver96, Section 3.1] is sufficient for Lemma 2 to hold. The definitions of the Clément interpolation operator, of the exact residuals and of the error estimator $\eta_{\mathrm{R},T}$ remain exactly the same as before. Only the definition of the approximate residuals is modified to accommodate the higher order approximation space. With these changes, the error bounds of Theorem 4 hold as before (but not uniformly with respect to the polynomial degrees k_1 and k_2).

Higher order ansatz functions for $V_{o,h}$ require changes of the theory only if the face residuals for interior faces can not be represented exactly by the approximate residuals, i.e. when $r_E \neq R_E$. Then the approximation term ζ_T has to include also terms for the interior faces.

5 Local problem error estimation

The key idea is to solve the problem locally with a higher accuracy. The difference to the original (piecewise linear) solution serves as error estimator, cf. the textbooks [AO00, Ver96]. In [Ver98a] a local problem error estimator has been derived for the convection–diffusion problem on isotropic elements.

On anisotropic elements, local problem error estimators could be established for the Poisson problem [Kun01a] and a singularly perturbed reaction–diffusion problem [Kun01c]. Here we follow the ideas introduced in those works. It is interesting, however, that apparently one has to solve a *reaction–diffusion* problem to obtain error bounds for the *convection–diffusion* problem (1). If a local convection–diffusion problem is solved instead then the upper error bound becomes worse. This coincides with the isotropic counterpart (note that the first and third error bound of [Ver98a, Proposition 5.1] are not correct).

As before, in section 5.1 we analyse error bounds when u_h is piecewise linear, and the residuals are approximated by constant values. In section 5.2 we discuss the extension to higher order approximations.

5.1 Error estimation using constant approximate residuals

Consider an arbitrary tetrahedron T. We start by defining a local, finite dimensional space V_T that consists of an element bubble function and some squeezed face bubble functions,

$$V_T := \operatorname{span}\{b_T, b_{E,\gamma_E} : E \subset \partial T \setminus \Gamma_{\mathrm{D}}\} \quad . \tag{27}$$

For interior tetrahedra this implies $\dim V_T = 5$. The squeezing parameters γ_E of the squeezed face bubble functions are now specified as in (26) to be

$$\gamma_E \;:=\; \min\left\{1\,,\; \frac{h_{min,E}}{h_E}\,,\; \frac{\varepsilon^{1/2}}{c_0^{1/2} h_E}\right\}$$

which implies $\gamma_E \sim \varepsilon^{1/2} h_E^{-1} \alpha_E$. Note that V_T depends implicitly on these parameters γ_E.

The local problem contains a new bilinear form that corresponds to a *reaction–diffusion* problem,

$$\tilde{B}(v,w) := \varepsilon(\nabla v, \nabla w) + c_0(v,w) \quad .$$

This bilinear form is elliptic and continuous, i.e.

$$\tilde{B}(v,v) = |||v|||^2\,, \qquad \tilde{B}(v,w) \le |||v||| \cdot |||w||| \quad .$$

The local problem and the error estimator are defined as follows.

Definition 3 (Local Dirichlet problem error estimator)
Find the unique solution $e_T \in V_T$ of the local variational problem:

$$\tilde{B}(e_T, v_T) \;=\; \sum_{T' \subset \omega_T} (r_{T'}, v_T)_{T'} \;+\; \sum_{E \subset \partial T \setminus \Gamma_{\mathrm{D}}} (r_E, v_T) \qquad \forall\, v_T \in V_T \quad . \tag{28}$$

The local *and* global error estimators *then become*

$$\eta_{\mathrm{D},T} := |||e_T|||_{\omega_T} \qquad \textit{and} \qquad \eta_{\mathrm{D}}^2 := \sum_{T \in \mathcal{T}} \eta_{\mathrm{D},T}^2 \quad . \tag{29}$$

The next lemma provides key properties of the local space V_T. Although the inequalities resemble the inverse inequalities of Lemma 2, the relations here are much more technical to obtain since a whole *space* of functions is involved (instead of just a single function).

Lemma 5 *The following relations hold for all $v_T \in V_T$.*

$$\begin{aligned} \|v_T\|_{\omega_T} &\lesssim h_{min,T} \cdot \|\nabla v_T\|_{\omega_T} \\ \|v_T\|_E &\lesssim h_E^{-1/2}\, \gamma_E^{-1/2} \cdot \min\{h_{min,T}, \gamma_E\, h_E\} \cdot \|\nabla v_T\|_{\omega_T} \qquad \forall\, E \subset \partial T \quad . \end{aligned}$$

If T has at least two Neumann boundary faces then the inequality constants can depend on the shape of the Neumann boundary (but not on T or $\mathcal{T}$).

Proof: The technical proof is given in [Kun01c]. ∎

Lemma 6 (Equivalence with residual estimator) *The local problem error estimator and the residual error estimator are locally equivalent in the following sense.*

$$\eta_{\mathrm{D},T}^2 \lesssim \sum_{T' \subset \omega_T} \eta_{\mathrm{R},T'}^2 \tag{30}$$

$$\eta_{\mathrm{R},T}^2 \lesssim \sum_{T' \subset \omega_T} \eta_{\mathrm{D},T'}^2 \quad . \tag{31}$$

If T has at least two Neumann boundary faces then the constant in (30) can depend on the shape of the Neumann boundary (but not on T or $\mathcal{T}$).

Proof: Recall first that the (element and face) residuals are approximated by constant values. Then both estimators depend only on these constant values, on the geometry of the elements of the patch ω_T, and on ε, c_0. It is important to note that the underlying differential equation (1) does *not* influence either estimator explicitly (it determines only the residuals).

For this reason we can proceed almost identically as in [Kun01c, Theorem 4.3] where the equivalence of the estimators has been proven. Note that this result relies heavily on Lemma 5. ∎

The main theoretical result for the local problem error estimator is presented next. The error bounds are the same as for the residual error estimator. Hence we can draw identical conclusions about reliability and efficiency of the estimator, cf. Section 4.

Theorem 7 (Local Problem error estimation) *The error is bounded locally from below for all $T \in \mathcal{T}$ by*

$$\eta_{\mathrm{D},T} \lesssim |||u - u_h|||_{\omega_T} \cdot \left(\max\{1, c_0^{-1}\|c\|_{\infty,\omega_T}\} + \varepsilon^{-1/2}\alpha_T\|\underline{b}\|_{\infty,\omega_T}\right) + \zeta_T \quad . \tag{32}$$

This lower bound can be rewritten again in the slightly weaker

$$\eta_{\mathrm{D},T} \lesssim |||u - u_h|||_{\omega_T} \cdot \left(\max\{1, c_0^{-1}\|c\|_{\infty,\omega_T}\} + \mathrm{Pe}_{\omega_T}\right) + \zeta_T \quad .$$

Assume further that the stabilization parameters satisfy $\delta_T \lesssim h_{min,T}/\|\underline{b}\|_{\infty,T}$. Then the error is bounded globally from above by

$$|||u - u_h||| \lesssim m_1(u - u_h, \mathcal{T}) \cdot \left[\eta_{\mathrm{D}}^2 + \zeta^2\right]^{1/2} \quad . \tag{33}$$

If T has at least two Neumann boundary faces then the constant in (32) can depend on the shape of the Neumann boundary (but not on T or $\mathcal{T}$).

Proof: The upper error bound follows immediately from the equivalence (31) of both estimators and the upper error bound (24) of the residual estimator.

The proof of the lower error bound (32) starts with a reformulation of the local problem (28). By element–wise partial integration one obtains the following equation that contains both bilinear forms $\tilde{B}$ and B: Find $e_T \in V_T$ such that

$$\tilde{B}(e_T, v_T) \;=\; B(u-u_h, v_T) + \sum_{T'\subset\omega_T} (r_{T'} - R_{T'}, v_T)_{T'} + \sum_{E\subset\partial T\cap\Gamma_N} (r_E - R_E, v_T)_E \qquad \forall\, v_T \in V_T.$$

Inserting $v_T = e_T$ and using the bound (5) for B, we derive

$$\begin{aligned}
|||e_T|||_{\omega_T}^2 &= \tilde{B}(e_T, e_T) \\
&= B(u-u_h, e_T) + \sum_{T'\subset\omega_T} (r_{T'} - R_{T'}, e_T)_{T'} + \sum_{E\subset\partial T\cap\Gamma_N} (r_E - R_E, e_T)_E \\
&\overset{(5)}{\le} |||u-u_h|||_{\omega_T} \cdot \left(\max\{1, c_0^{-1}\|c\|_{\infty,\omega_T}\}\, |||e_T|||_{\omega_T} + \varepsilon^{-1/2}\|\underline{b}\|_{\infty,\omega_T}\|e_T\|_{\omega_T}\right) \\
&\quad + \left(\sum_{T'\subset\omega_T} \|r_{T'} - R_{T'}\|_{T'}^2\right)^{1/2} \|e_T\|_{\omega_T} + \sum_{E\subset\partial T\cap\Gamma_N} \|r_E - R_E\|_E\, \|e_T\|_E \quad .
\end{aligned}$$

Next we bound $\|e_T\|_{\omega_T}$ and $\|e_T\|_E$. The following inequalities can be proven using Lemma 5 (alternatively they have already been derived in the proof of [Kun01c, Theorem 4.3]). For the local space V_T with the specific choice of γ_E, one obtains for all functions $v_T \in V_T$

$$\begin{aligned}
\|v_T\|_{\omega_T} &\lesssim \alpha_T\, |||v_T|||_{\omega_T} \\
\|v_T\|_E &\lesssim \varepsilon^{-1/4}\alpha_T^{1/2}\, |||v_T|||_{\omega_T} \quad .
\end{aligned}$$

Substitute again $v_T = e_T$, combine all inequalities and recall $|||e_T|||_{\omega_T} = \eta_{D,T}$ to obtain the desired lower error bound. ∎

Remark 3 The local problem for the definition of the error estimator is a *reaction–diffusion* problem. It is remarkable that the seemingly natural choice of a *diffusion–convection–reaction* local problem does not yield an equivalence to the residual error estimator. As a consequence, an upper error bound such as (33) does not hold.

This behaviour is independent of the anisotropy of the elements and is seen also for isotropic elements (note that the isotropic result of [Ver98a, Proposition 5.1] is partially wrong). □

5.2 Error estimation using higher order approximate residuals

When higher order approximate residuals are employed, roughly the same arguments as in section 4.2 apply. Some aspects, however, are considerably more technical here.

For a precise description assume again $r_T \in \mathbb{P}^{k_1}(T)$ and $r_E \in \mathbb{P}^{k_2}(E)$. Then the local space $V_T \equiv V_T^{k_1,k_2}$ has to contain all functions $b_T\,\varphi_T$ and $b_{E,\gamma_E}\,F_{ext}(\varphi_E)$, with $\varphi_T \in \mathbb{P}^{k_1}(T)$, $\varphi_E \in \mathbb{P}^{k_2}(E)$. Moreover the extension operator F_{ext} should be improved such that $F_{ext}(r_E)$

is independent of the local enumeration of the vertices of T (this is not the case with the choice of [Ver96, Section 3.1]).

The most severe theoretical difficulty stems from Lemma 5. Even the proof for constant approximate residuals (corresponding to $V_T^{k_1,k_2}$ with $k_1 = k_2 = 0$) in [Kun01c] is very technical. The situation is likely to become worse for higher order approximations.

From a practical point of view, the efficient implementation of the local problem requires additional consideration. The computational expense will heavily increase with higher k_1, k_2, cf. again [Kun01c]. Hence one has to find a balance between accuracy and implementational and computational cost.

6 Numerical experiments

The following three experiments will underline and confirm the theoretical predictions. The first and easiest example features a convection–diffusion problem with vanishing convection (i.e. the simpler reaction–diffusion problem). The second example describes a convection–diffusion problem with exponential boundary layers. The third example is the most difficult one; the underlying convection–diffusion equation gives rise to a parabolic boundary layer.

We present the main theoretical results for the residual error estimator η_{R}, cf. Theorem 4 of section 4. In all examples we consider four values of the perturbation parameter, namely $\varepsilon = 10^{-1}, 10^{-2}, 10^{-3}, 10^{-6}$. The methodology to investigate the quality of the solution process and of the error estimation is described in detail in Section 6.1 and repeated subsequently.

6.1 Example 1

The reaction–diffusion problem described here is the special case of the convection–diffusion problem (1) with vanishing convection. Although this example does not feature 'dominating convection', we have included it since it allows us to distinguish between effects that are due to the anisotropic discretisation, and effects that are caused by a large convection.

In this example the local mesh Peclet number vanishes; $\mathrm{Pe}_T = 0$ for all elements $T \in \mathcal{T}$. This favourite property implies that the corresponding variational problem and the discrete problem are symmetric, respectively, and can be solved without stabilisation ($\delta_T = 0 \, \forall T \in \mathcal{T}$). Note that similar investigations in 3D can be found in [Kun01b, Kun01c]; for 2D results see [HL98, Ex. 4.2]. Here we have included this example to have a comparison with problems with non–vanishing convection.

With $\underline{b} = (0,0)^\top$ and $c = c_0 = 1$ the PDE becomes

$$-\varepsilon \Delta u + u \;=\; 0 \qquad \text{in } \Omega = (0,1)^2 \qquad .$$

The exact solution is prescribed to be

$$u := \mathrm{e}^{-x/\sqrt{\varepsilon}} + \mathrm{e}^{-y/\sqrt{\varepsilon}}$$

and exhibits exponential boundary layers of width $\mathcal{O}(\sqrt{\varepsilon}|\ln\varepsilon|)$ along the lines $x = 0$ and $y = 0$. The Dirichlet boundary data on $\Gamma_D := \partial\Omega$ are set accordingly.

We utilize a sequence of three–directional triangular Shishkin type meshes. More precisely, the 2D mesh is the tensor product of two 1D Shishkin type meshes with transition point $\tau := \min\{1/2, \sqrt{\varepsilon} \cdot |\ln\varepsilon|\}$.

Figure 4 presents the decrease of the error in the energy norm. The optimal rate of convergence of approximately $|||u - u_h||| = \mathcal{O}(\mathrm{DoF}^{-0.5})$ confirms that the chosen meshes are appropriate to resolve the boundary layers. Judging from our experience in [Kun99, Kun01b] we expect the matching function $m_1(u - u_h, \mathcal{T})$ to be of moderate size, i.e. in the range of $2 \ldots 4$.

Additionally in Figure 4 we display the global error estimator η_R which always overestimates the error by a factor of about 5.

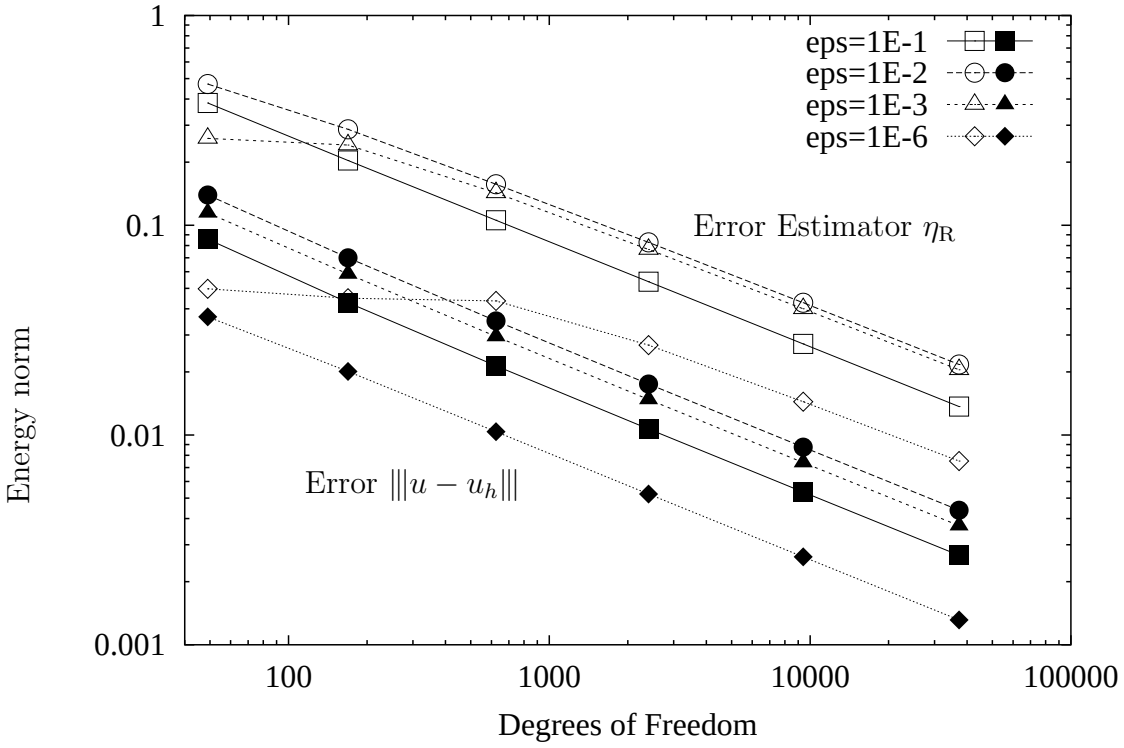

Figure 4: Error $|||u - u_h|||$ (filled symbols)
Error estimator η_R (empty symbols)

Next we investigate the main theoretical results which are the upper and lower error bounds of Theorem 4. In order to present the underlying inequalities (24) and (22) appropriately, we reformulate them by defining the ratios of left–hand side and right–hand side, respectively:

$$q_{\mathrm{up}} := \frac{|||u - u_h|||}{[\eta_R^2 + \zeta^2]^{1/2}}$$

$$q_{\text{low}} \;:=\; \max_{T\in\mathcal{T}} \frac{\eta_{\mathrm{R},T}}{|||u-u_h|||_{\omega_T}\cdot\left(\max\{1,c_0^{-1}\|c\|_{\infty,\omega_T}\}+\varepsilon^{-1/2}\alpha_T\|\underline{b}\|_{\infty,\omega_T}\right)\;+\;\zeta_T} \quad .$$

The first ratio q_{up} (or its inverse) is frequently referred to as *effectivity index* and measures the *reliability* of the estimator. The second ratio is related to the *efficiency* of the estimator.

Note further that the factor in the denominator of q_{low} simplifies to

$$\max\{1,c_0^{-1}\|c\|_{\infty,\omega_T}\}+\varepsilon^{-1/2}\alpha_T\|\underline{b}\|_{\infty,\omega_T}\equiv 1$$

for this first example since $\underline{b}=(0,0)^\top$. Additionally the approximation terms vanish, $\zeta_T=\zeta=0$.

The lower and upper error bound (22), (24) now correspond to

$$q_{\text{low}} \;\lesssim\; 1 \qquad \text{and} \qquad q_{\text{up}} \;\lesssim\; m_1(u-u_h,\mathcal{T}) \quad .$$

In the right part of Figure 5 we observe indeed that q_{low} is bounded from above by 2.0. Hence the estimator is *efficient*.

In order to investigate the upper error bound, recall first that the matching function $m_1(u-u_h,\mathcal{T})$ is expected to be of moderate size $(2\ldots4)$ since we employ well adapted meshes. Hence the corresponding ratio q_{up} should be bounded from above which is confirmed by the experiment (left part of Figure 5). As soon as a reasonable resolution of the layer is achieved, the quality of the upper error bound is independent of ε. Thus the estimator is also *reliable*.

Finally we note that the qualitative and the quantitative behaviour of the error estimator is very similar to the 3D counterpart, as described in [Kun01b].

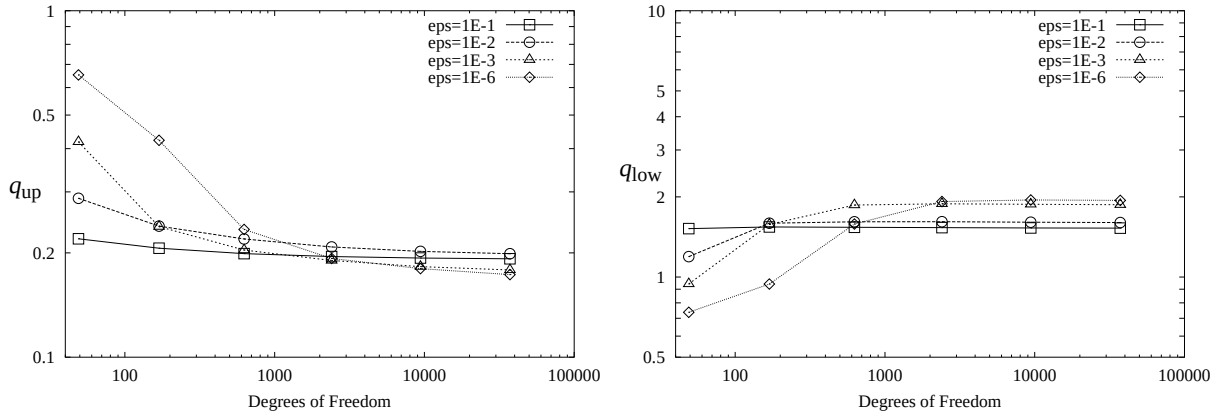

Figure 5: Left: Upper error bound q_{up}
Right: Lower error bound q_{low}

6.2 Example 2

The second example is a typical convection–diffusion problem. It involves convection along $\underline{b} = (b_1, b_2)^\top = (2, 3)^\top$, and we set $c = c_0 = 1$. For the resulting PDE

$$-\varepsilon\Delta u \;+\; 2u_x + 3u_y \;+\; u \;=\; f \qquad \text{in } \Omega = (0,1)^2$$

we prescribe the analytical solution

$$u = \sin(x)(1 - \mathrm{e}^{-2(1-x)/\varepsilon}) \cdot y^2(1 - \mathrm{e}^{-3(1-y)/\varepsilon}) \qquad .$$

The right–hand side f and the Dirichlet boundary data on $\partial\Omega$ are chosen accordingly.

The solution shows exponential boundary layers along the outflow boundary at $x = 1$ and $y = 1$. This choice of u serves as a typical example for boundary layers that are caused by incompatibilities of f and the boundary data.

Similar to the previous example we employ a three–directional 2D Shishkin mesh. With N denoting the number of nodal points in x and y direction, the mesh transitions points are placed at

$$\tau_x := \min\{1/2, 2\varepsilon \ln N/b_1\} \qquad , \qquad \tau_y := \min\{1/2, 2\varepsilon \ln N/b_2\} \qquad ,$$

respectively, cf. [LS01, Section 2.2]. Hence inside the layer region the local mesh Peclet number is small, $\mathrm{Pe}_T \sim 1$.

The unsymmetric variational problem requires stabilisation to yield accurate results. For the stabilisation parameter δ_T we follow the isotropic proposal in [Ver98a] and define the anisotropic counterpart by

$$\delta_T := \frac{h_{min,T}}{2\|\underline{b}\|_{\infty,T}} \cdot (\coth(\mathrm{Pe}_T) - \mathrm{Pe}_T^{-1}) \qquad .$$

This implies little stabilisation in the layer region and comparatively large stabilisation in the coarse mesh region.

The results are presented in a similar fashion as for example 1. Start with the decrease of the error $|||u - u_h|||$ and the error estimator, respectively, which is depicted in Figure 6. The convergence rate is approximately $|||u - u_h||| = \mathcal{O}(\mathrm{DoF}^{-0.41})$ and thus sub–optimal. The error estimator η_{R} overestimates the error by a factor of approximately 5 but behaves similarly otherwise.

In order to assess the error bounds, we compute again the ratios q_{low} and q_{up} and present them in Figure 7, cf. the previous example. Starting with the lower error bound (22), we observe that q_{low} is indeed bounded from above which confirms the theoretical predictions. Note, however, that the right–hand side of (22) now contains the factor $\max\{1, c_0^{-1}\|c\|_{\infty,\omega_T}\} + \varepsilon^{-1/2}\alpha_T\|\underline{b}\|_{\infty,\omega_T}$. This additional factor is of order 1 for small mesh Peclet numbers $\mathrm{Pe}_T \lesssim 1$, i.e. for elements inside the layer region. Then the error estimator is *efficient*.

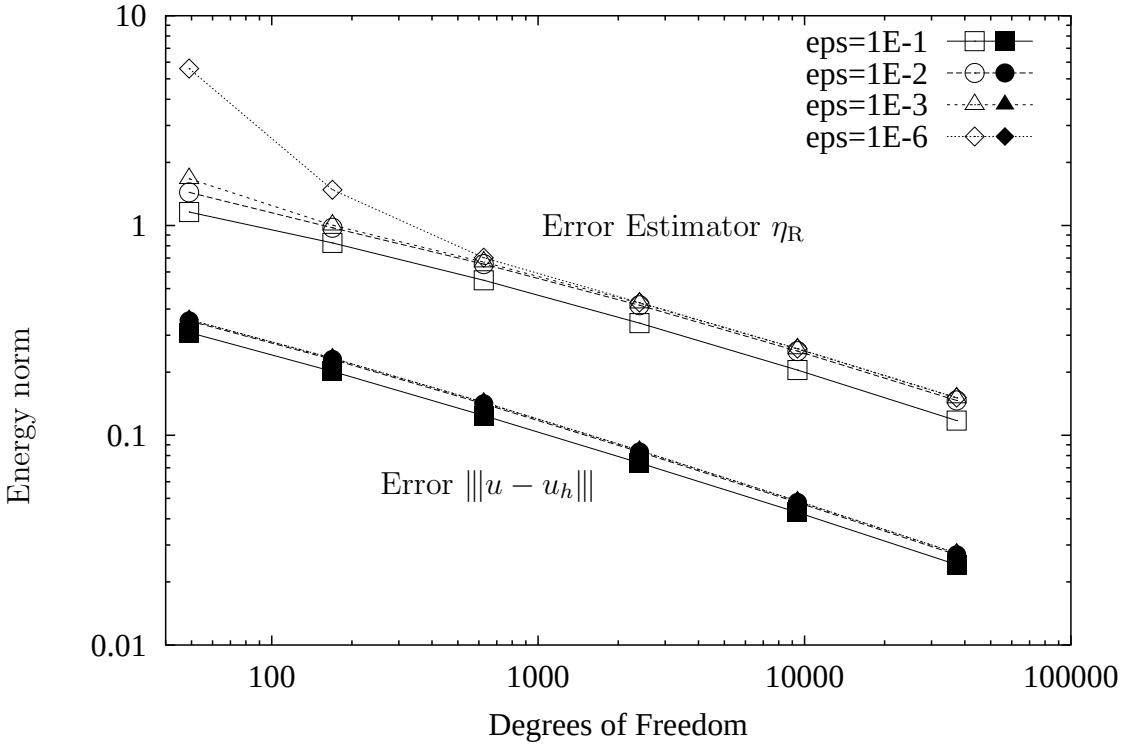

Figure 6: Error $|||u - u_h|||$ (filled symbols)
Error estimator η_R (empty symbols)

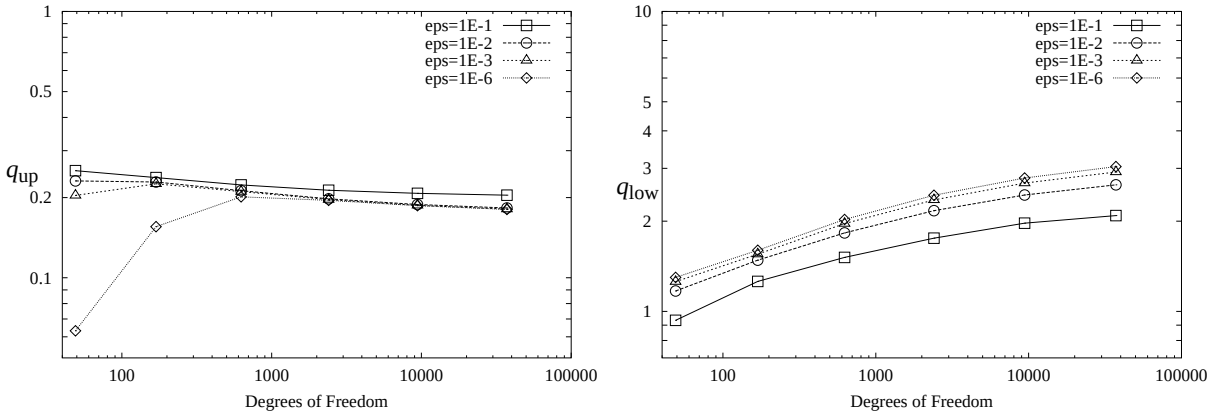

Figure 7: Left: Upper error bound q_{up}
Right: Lower error bound q_{low}

Conversely, the aforementioned factor becomes large for elements with a large mesh Peclet number $\mathrm{Pe}_T \gg 1$, i.e. in the coarse mesh region. Numerical investigation strongly suggests that this factor cannot be omitted. As a consequence the efficiency of the error estimator deteriorates as Pe_T becomes large. On the other hand this may not be too much of a disadvantage since the mesh Peclet number should be large only in regions where the solution u is smooth and the error is already small.

When investigating the upper error bound (24), the corresponding ratio q_{up} is bounded by the matching function $m_1(u - u_h, \mathcal{T})$. Again we expect m_1 to be of moderate size (say $2 \ldots 4$). Hence q_{up} has to bounded from above which is confirmed by the left part of Figure 7. Consequently the error estimator is *reliable*.

6.3 Example 3

This example features a so–called parabolic layer. The numerical comparison of [Joh00] reveals that such layers are much more difficult to treat than exponential layers, in particular when designing adaptive algorithms. The theoretical knowledge is also less developed although parabolic layers may be equally important in practical applications. The difficulties become apparent in the experiment below.

Our test is largely inspired by [HL98, Example 4.3]. With $\underline{b} = (1, 0)^\top$ and $c = c_0 = 1$ the PDE becomes

$$-\varepsilon \Delta u + u_x + u \;=\; f \qquad \text{in } \Omega = (0,1)^2 \qquad .$$

The exact solution is prescribed to be

$$u = \frac{1}{\sqrt{1+x}} \cdot \exp\Big(- \frac{y^2}{4\varepsilon(1+x)} \Big)$$

with an appropriate right–hand side f and the Dirichlet boundary data on $\partial\Omega$. This solution u displays a typical parabolic layer along the line $y = 0$. Note that the layer width of $\mathcal{O}(\sqrt{\varepsilon})$ is much larger than for an exponential layer.

Again a three–directional 2D Shishkin mesh is employed. With N denoting the number of nodal points in y direction, the mesh transition point is set to

$$\tau := \min\{1/2, 2\sqrt{\varepsilon} \ln N\}$$

Hence the elements T in the layer region have a minimal dimension $h_{min,T} \sim \sqrt{\varepsilon}$ which is (much) larger than ε (unless the mesh is very fine which is unrealistic for small ε). Consequently the local mesh Peclet number is (much) larger than 1 *even in the critical layer region*. This observation is a key difference to the exponential layers (cf. example 2).

When solving the variational problem, we apply the stabilisation proposed in [HL98, Section 3.3] (up to the factor 1/3), namely

$$\delta_T = \frac{h_{min,T}}{3\|\underline{b}\|_{\infty,T}} \cdot \min\{1, \mathrm{Pe}_T\} \qquad .$$

With this setting the convergence rate of the error $|||u - u_h|||$ in the energy norm is $\mathcal{O}(\mathrm{DoF}^{-0.50})$ for $\varepsilon = 10^{-1}$ and drops to about $\mathcal{O}(\mathrm{DoF}^{-0.40})$ for $\varepsilon = 10^{-6}$. The error estimator η_{R} behaves qualitatively similarly and overestimates the error as in the previous example.

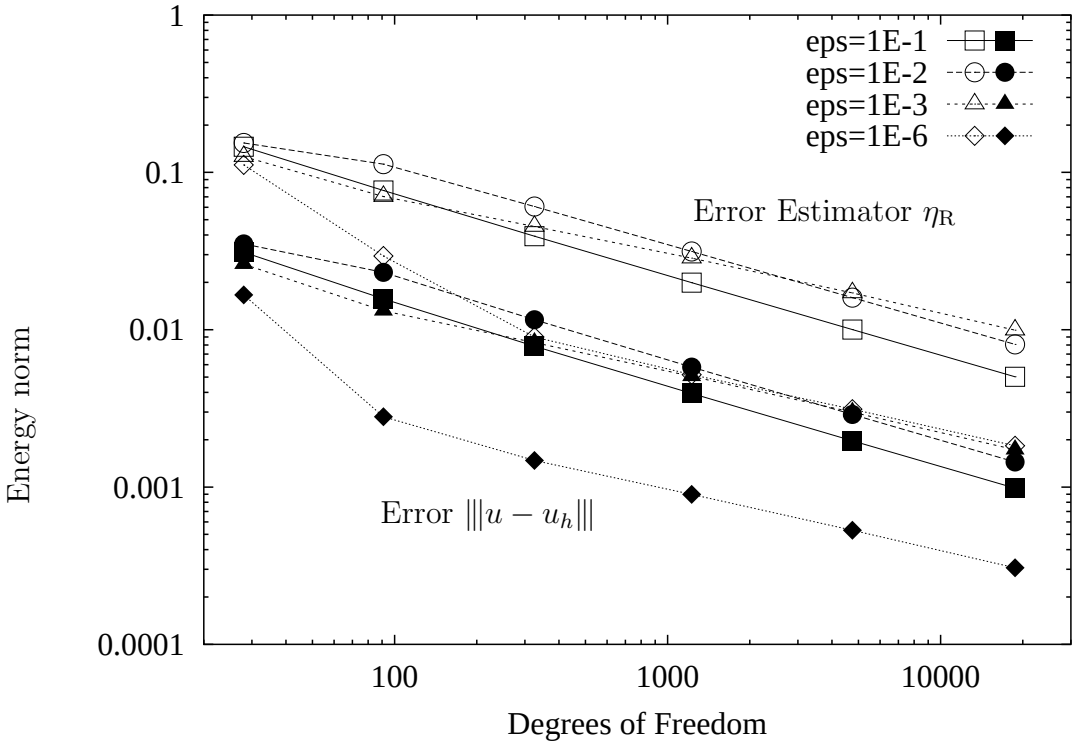

Figure 8: Error $|||u - u_h|||$ (filled symbols)
Error estimator η_{R} (empty symbols)

Next we investigate the error bounds in Figure 9. For the lower error bound (22) we compute again q_{low}. In accordance with the theory, q_{low} is bounded from above. Since most values of q_{low} are much smaller than in previous examples, the error bound (22) is not sharp here. This may be caused by the parabolic structure of the boundary layer.

A more detailed inspection reveals that the *efficiency* is lost only for coarse mesh elements, i.e. where the mesh Peclet number is large. Inside the parabolic layer the mesh Peclet number is still large (unless the mesh is unrealistically fine for small ε). Nevertheless the numerical results for this example yield that the error estimator is still quite efficient, with only a mild decrease of efficiency for small ε and fine meshes. This behaviour is somewhat better than we can expect from the theory.

The upper error bound is presented in the left part of Figure 9. This upper bound (24) is not influenced by a (large) mesh Peclet number Pe_T, which should be reflected in the numerical behaviour. Indeed we notice the same performance as in the previous example, i.e. q_{up} is bounded from above, and hence the error estimator is *reliable*. No adverse

influence on the reliability is seen that could stem from large values of Pe_T.

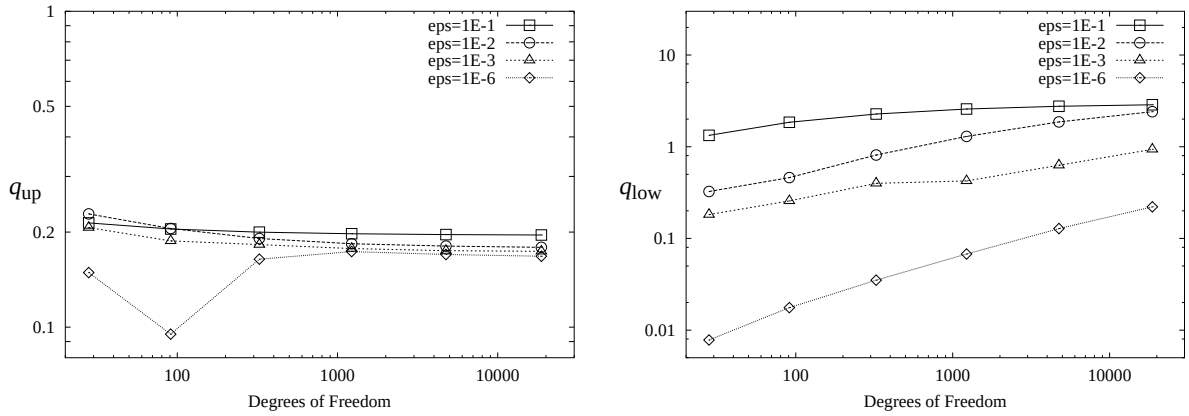

Figure 9: Left: Upper error bound q_{up}
Right: Lower error bound q_{low}

6.4 Anisotropic stabilisation parameter

In order to avoid numerical instabilities when solving the singularly perturbed convection–diffusion problem (1) one often resorts to stabilisation techniques, such as the SUPG approach (6) discussed here. An important question then is the correct choice of the stabilisation parameter δ_T. For *isotropic* meshes there are several proposals and theoretical investigations, see e.g. [RST96, Section III.3.2.1]. For *anisotropic* elements there is little knowledge about appropriate choices of the stabilisation parameter. Hence we present here existing proposals as well as some extensions of isotropic stabilisation parameters.

Hangleiter/Lube [HL98, Section 3.3] propose

$$\delta_T = \frac{h_{min,T}}{3\|\underline{b}\|_{\infty,T}} \cdot \min\{1, \mathrm{Pe}_T\}$$

although they do not specify the factor 1/3. This factor worked sufficiently well for our examples.

The isotropic version of Verfürth [Ver98a, Section 7] can be generalized to

$$\delta_T = \frac{h_{min,T}}{2\|\underline{b}\|_{\infty,T}} \cdot (\coth(\mathrm{Pe}_T) - \mathrm{Pe}_T^{-1}) \quad .$$

Similarly the isotropic stabilisation of Kay/Silvester [KS01, Section 2.1] is extended to

$$\delta_T = \frac{h_{min,T}}{2\|\underline{b}\|_{\infty,T}} \cdot (1 - \min\{1, \mathrm{Pe}_T^{-1}\}) \quad .$$

Finally there is a proposal by Linß/Stynes [LS01, Section 2.3] for Shishkin meshes which reads

$$\delta_T \sim \begin{cases} h_{min,T} & \text{if } \mathrm{Pe}_T \geq 1 \\ 0 & \text{if } \mathrm{Pe}_T < 1 \end{cases} .$$

For the first three choices we also present graphically the dependence of δ_T on the local mesh Peclet number Pe_T. To this end we omit the common factor $h_{min,T}/(2\|\underline{b}\|_{\infty,T})$, i.e. we investigate the term $\delta_T \cdot 2\|\underline{b}\|_{\infty,T}/h_{min,T}$. Figure 10 shows the behaviour for small and medium values of Pe_T. We note that significant differences occur only for Pe_T in the range of about $0 \ldots 2$ (which usually corresponds to elements in or near exponential layer regions).

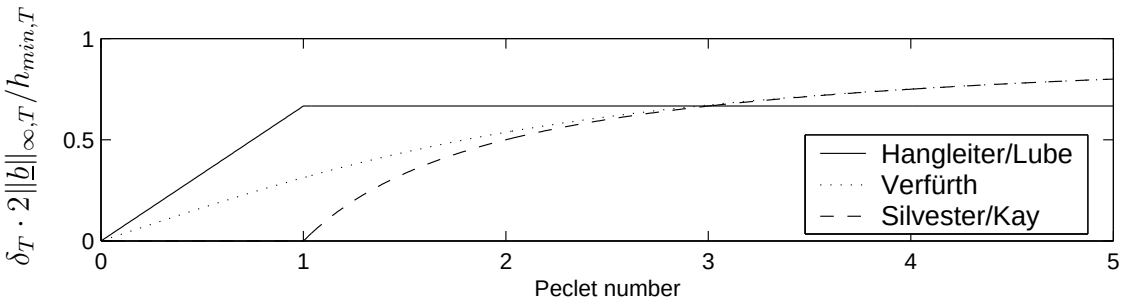

Figure 10: Dependence of stabilisation parameter δ_T on Peclet number Pe_T

There is the natural question which stabilisation performs best, i.e. which method yields the smallest error in the energy norm. First experiments with anisotropic meshes indicate that the differences are quite small. For fine meshes the different stabilisations are almost undistinguishable for certain examples. Slightly surprising, even omitting the stabilisation produces the same results. The reason could be that numerical oscillations in the solution may be avoided in two ways, either by using stabilisation or by using solution adapted (anisotropic) meshes.

In order to visualize the aforementioned observation we consider again example 2 but now *without stabilisation*, i.e. $\delta_T = 0$. In a similar fashion as before we present in Figure 11 the error $|||u - u_h|||$ in the energy norm and the error estimator η_{R}.

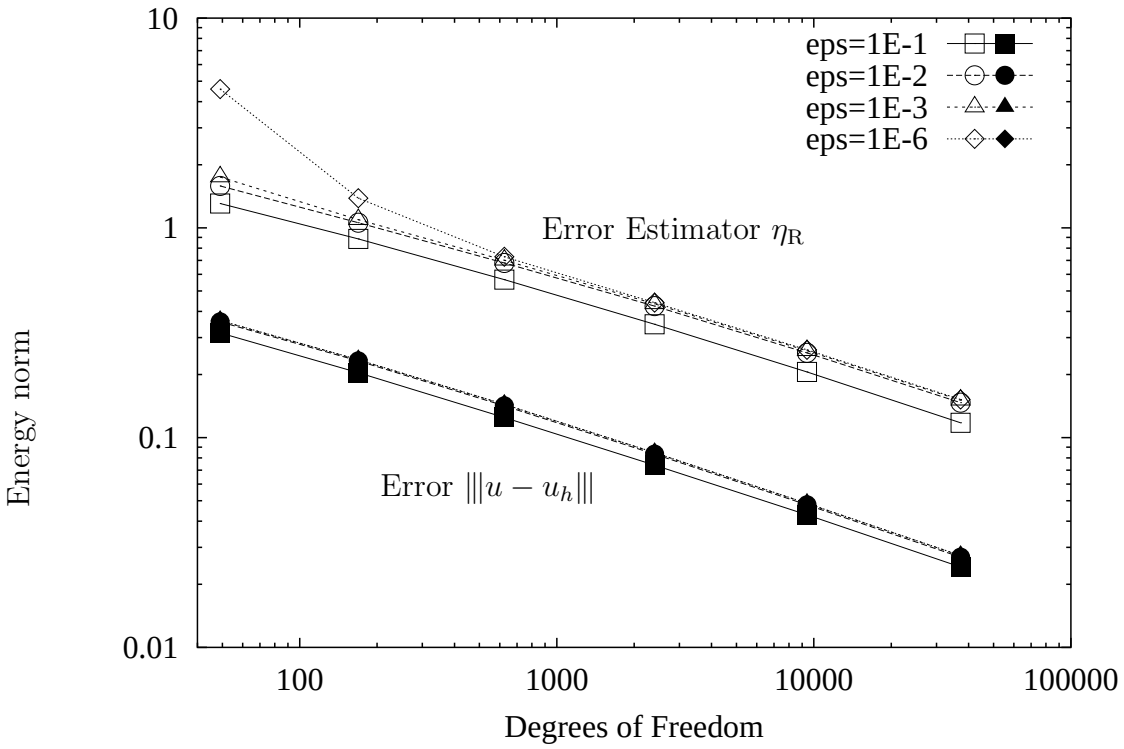

Figure 11: Error $|||u - u_h|||$ (filled symbols)
Error estimator η_R (empty symbols)

Next the results for the lower and upper error bounds (22), (24) are given in Figure 12. The differences to the figures of example 2 are rarely visible, and we can refer to the same conclusions.

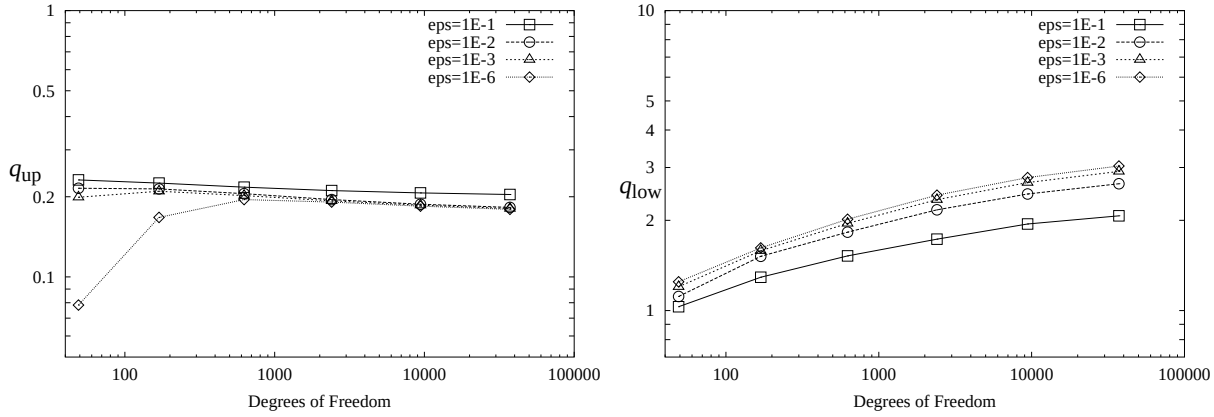

Figure 12: Left: Upper error bound q_{up}
Right: Lower error bound q_{low}

We remark that the different stabilisations perform similarly only with respect to the error in the *energy norm*. If one is interested in the error in the (discrete) *maximum norm* then the differences are much more pronounced.

Summarizing, stabilisation is vitally important for isotropic meshes but not fully understood for anisotropic elements. There are indications that for appropriate anisotropic meshes little or no stabilisation is necessary.

6.5 Remarks

Some remarks may be useful and complement the numerical experiments. Let us start with accuracy matters. All error integration has been performed with a 7 point numerical integration rule of order 5. Tests with a 16 point integration rule of order 8 confirm a sufficient accuracy. This could be expected for our examples since layers are properly resolved.

In the last section we have investigated the influence of the stabilisation. The quality of the solution is also determined by the underlying mesh $\mathcal{T}$. This includes in particular

- the choice of the diagonals in a tensor product type mesh, i.e. whether a three–directional mesh or a criss–cross mesh is used,
- the choice of the transition parameter τ for Shishkin type meshes,
- the type of mesh that is used (e.g. Shishkin type mesh, Bakhvalov mesh, adaptively created meshes, ...).

It is clearly beyond the scope of this work to investigate all these factors in detail. We have carried out many more experiments than those presented. From this we deduce that the results may differ from that of the previous sections but the general conclusions about reliability and efficiency of the error estimator are the same.

7 Summary

We have considered a singularly perturbed convection–diffusion problem that is discretised using the SUPG stabilisation of the finite element method. The main focus has been on *a posteriori* error estimators that are suitable for *anisotropic* elements. Two estimators have been proposed, based either on the residuals or the solution of local problems.

The analysis has shown that the upper error bound depends on the alignment of the anisotropies of mesh and solution. Hence *reliable* error estimation is possible for suitably aligned anisotropic meshes. The lower error bound includes a local mesh Peclet number; the results obtained is analogous to isotropic meshes. Thus *efficient* error estimation is achieved for small Peclet numbers $\mathrm{Pe}_T \lesssim 1$.

Hence the existing theory of error estimators for isotropic meshes has been extended to anisotropic elements, and analogous reliability and efficiency results have been proven. The standard Galerkin FEM is covered as well. Numerical experiments have confirmed the analysis.

References

[Ada75] R. A. Adams. *Sobolev Spaces*. Academic Press, New York, 1975.

[Ang95] L. Angermann. Balanced a-posteriori error estimates for finite volume type discretizations of convection-dominated elliptic problems. *Computing*, 55(4):305–323, 1995.

[AO00] M. Ainsworth and J.T. Oden. *A posteriori error estimation in finite element analysis*. Wiley, 2000.

[Ape99] Th. Apel. *Anisotropic finite elements: Local estimates and applications*. Advances in Numerical Mathematics. Teubner, Stuttgart, 1999.

[Cia78] P. G. Ciarlet. *The finite element method for elliptic problems*. North-Holland, Amsterdam, 1978.

[Clé75] P. Clément. Approximation by finite element functions using local regularization. *RAIRO Anal. Numer.*, 2:77–84, 1975.

[DGP99] M. Dobrowolski, S. Gräf, and C. Pflaum. On a posteriori error estimators in the finite element method on anisotropic meshes. *Electronic Transactions Num. Anal.*, 8:36–45, 1999.

[FPZ01] L. Formaggia, S. Perotto, and P. Zunino. An anisotropic a-posteriori error estimate for a convection-diffusion problem. *Comput. Vis. Sci.*, 4(2):99–104, 2001.

[HL98] R. Hangleiter and G. Lube. Stabilized Galerkin methods and layer-adapted grids for elliptic problems. *Comput. Methods Appl. Mech. Eng.*, 166(1–2):165–182, 1998.

[Joh00] V. John. A numerical study of a posteriori error estimators for convection–diffusion equations. *Comput. Methods Appl. Mech. Engrg.*, 190:757–781, 2000.

[Kop01] N. Kopteva. Maximum norm a posteriori error estimates for a one-dimensional convection-diffusion problem. *SIAM J. Numer. Anal.*, 39(2):423–441, 2001.

[KS01] D. Kay and D. Silvester. The reliability of local error estimators for convection–diffusion equations. *IMA J. Numer. Anal.*, 21(1):107–122, 2001.

[Kun99] G. Kunert. *A posteriori error estimation for anisotropic tetrahedral and triangular finite element meshes*. Logos Verlag, Berlin, 1999. Also PhD thesis, TU Chemnitz, http://archiv.tu-chemnitz.de/pub/1999/0012/index.html.

[Kun00] G. Kunert. An a posteriori residual error estimator for the finite element method on anisotropic tetrahedral meshes. *Numer. Math.*, 86(3):471–490, 2000. DOI 10.1007/s002110000170.

[Kun01a] G. Kunert. A local problem error estimator for anisotropic tetrahedral finite element meshes. *SIAM J. Numer. Anal.*, 39(2):668–689, 2001.

[Kun01b] G. Kunert. Robust a posteriori error estimation for a singularly perturbed reaction–diffusion equation on anisotropic tetrahedral meshes. *Adv. Comp. Math.*, 15(1–4):237–259, 2001.

[Kun01c] G. Kunert. Robust local problem error estimation for a singularly perturbed problem on anisotropic finite element meshes. *Math. Model. Numer. Anal.*, 35(6):1079–1109, 2001.

[KV00] G. Kunert and R. Verfürth. Edge residuals dominate a posteriori error estimates for linear finite element methods on anisotropic triangular and tetrahedral meshes. *Numer. Math.*, 86(2):283–303, 2000. DOI 10.1007/s002110000152.

[LS01] T. Linss and M. Stynes. The SDFEM on Shishkin meshes for linear convection-diffusion problems. *Numer. Math.*, 87(3):457–484, 2001.

[Mor96] K. W. Morton. *Numerical solution of convection-diffusion problems*. Chapman & Hall, London, 1996.

[RST96] H.-G. Roos, M. Stynes, and L. Tobiska. *Numerical methods for singularly perturbed differential equations. Convection-diffusion and flow problems*. Springer, Berlin, 1996.

[San01] G. Sangalli. A robust a posteriori estimator for the Residual–free Bubbles method applied to advection-diffusion problems. *Numer. Math.*, 89(2):379–399, 2001.

[Sie96] K. G. Siebert. An a posteriori error estimator for anisotropic refinement. *Numer. Math.*, 73(3):373–398, 1996.

[Ver96] R. Verfürth. *A review of a posteriori error estimation and adaptive mesh–refinement techniques*. Wiley-Teubner, Chichester; Stuttgart, 1996.

[Ver98a] R. Verfürth. A posteriori error estimators for convection–diffusion equations. *Numer. Math.*, 80(4):641–663, 1998.

[Ver98b] R. Verfürth. Robust a posteriori error estimators for singularly perturbed reaction–diffusion equations. *Numer. Math.*, 78(3):479–493, 1998.